The Atlantic Testing Platform for Maritime Robotics

Topic	ICT-09-2019-2020 (H2020)
Acronym	ATLANTIS
Title	The Atlantic Testing Platform for Maritime Robotics: New Frontiers for Inspection and Maintenance of Offshore Energy Infrastructures.
Project number	871571
Delivery date	30.09.2023
Deliverable number	D4.4 (D16)
Dissemination level	Public
Lead Beneficiary	VTT

Results of the predictive maintenance centered on robotics use

VTT

Actions

	Action	Organisation	Date
Technical Manager	Requested deliverable from the Deliverable Responsible.	VTT	06.09.2023
Deliverable Responsible	Prepared draft of the deliverable.	VTT	20.09.2023
Technical Manager	Approved the updated draft as the first version.	VTT	20.09.2023
Quality Manager	Approved the updated first version as the second version.	UdG	28.09.2023
Project Coordinator	Approved the updated second version as the final version and sent to the European Commission.	INESC TEC	29.09.2023

Disclaimer

This project has received funding from the European Union's Horizon 2020 research and innovation programme, under the Grant Agreement no. 871571.

Abbreviations

AWP	Waterplane area
B_{crit}	Critical Damping
BM	Metacentric radius
B_{visc}	Viscous Damping
CTB	Coastal Testbed
DAQ	Data acquisition
Dir	Wave propagating direction
g	Gravitational acceleration
GM	Metacentric height
Hs	Significant Wave Height
IMR	Inspection, maintenance and repair
KB	Height of center of buoyance above the keel
KG	Height of center of gravity above the keel
Kxx	Radius of gyration about x-axis
Kyy	Radius of gyration about y-axis
Kzz	Radius of gyration about z--axis
O&M	Operation and maintenance
PdM	Predictive maintenance
RMS	Root mean square
RX	Roll - Rotation around x-axis
RY	Pitch - Rotation around y-axis
RZ	Yaw - Rotation around z-axis
SCC	Supervisory Control Center
TAL	Time-at-Level
Tp	Peak Period
X	Surge - Translation along x-axis
Y	Sway - Translation along y-axis
Z	Heave - Translation along z-axis
ZB	Vertical position of center of buoyance referred to a reference axis system
ZG	Vertical position of center of gravity referred to a reference axis system

This project has received funding from the European Union's Horizon 2020 research and innovation programme, under the Grant Agreement no. 871571.

Contents

This project has received funding from the European Union's Horizon 2020 research and innovation programme, under the Grant Agreement no. 871571.

1. Introduction

1.1. Scope of work

This report presents predictive maintenance tools for offshore wind in the context of the ATLANTIS Test Center. Tools for

1. Mooring line maintenance need assessment and
2. Operational window assessment for structural maintenance

were developed based on data and a virtual model of the ATLANTIS Coastal Testbed. The virtual model represents the Coastal Testbed floating structure, a cylindrical buoy that is moored to the harbour in Viana do Castelo. The analysed environmental conditions however, represent conditions at the Atlantic Ocean on the coast of Portugal and are similar to the ones at the WindFloat Atlantic (the ATLANTIS Offshore Testbed). Thus, all the simulated data represent this site-specific sea state.

1.2. Main objectives

The main objectives of this work are to

1. Provide support for deterministic decision making on when and where to deploy robots for inspections and maintenance based on stochastic loading analytics.

2. Help determine operational windows for human and robotic-based inspections considering motions of the structure in different weather conditions and the defined inspection and maintenance need.

1.3. Structure of the document

The document consists of five parts.

1. Introduction: This section describes the scope, objectives and structure of the document.

2. Coastal Testbed Digital Twin: This section describes the virtualization of the Coastal Testbed floating structure using measured motion data and wave conditions for the Portugal coast. The digital twin is used to model the motions of the structure as well as structural and mooring line loads in different sea states.

3. Predictive maintenance with O&M module: This section describes i) the analysis of operational windows for O&M actions based on motions of the floating structure and ii) mooring line lifetime and maintenance need assessment as an example case of predictive maintenance.

4. The O&M toolbox as a part of robotic-based IMR: This section describes the use of the analysis tools presented in section 3 for robotic-based IMR.

5. Conclusions: This section summarizes the work done and its applicability to robotic-based IMR.

This project has received funding from the European Union's Horizon 2020 research and innovation programme, under the Grant Agreement no. 871571.

2. Coastal Testbed Digital Twin

2.1. Measurements at the floating structure

2.1.1. Instrumentation

The Coastal Testbed floating structure DURIUS was instrumented with an external measurement system including accelerometers, a state of motion sensor, a wind sensor, a wave buoy, and cameras, see Figure 2-1. The instrumentation was carried out in August/September 2022 by VTT personnel (supported by INESC TEC team) and by using VTT's measurement sensors and systems. The setup functioned as an external DAQ system running separately on the Testbed edge 24/7. The measurement system was located both on the Coastal Testbed structure, its close vicinity, and the pier (see Figures 2-1 – 2-3). There were three 3D vibration acceleration sensors and one state of motion sensor on the floating Testbed structure for measuring movements. Waves were monitored with a camera and a wave buoy measurement unit. Wind direction and speed were measured with a wind sensor installed on the structure. The sensors and the corresponding measurement frequencies are listed in Tables 2-1 and 2-2.

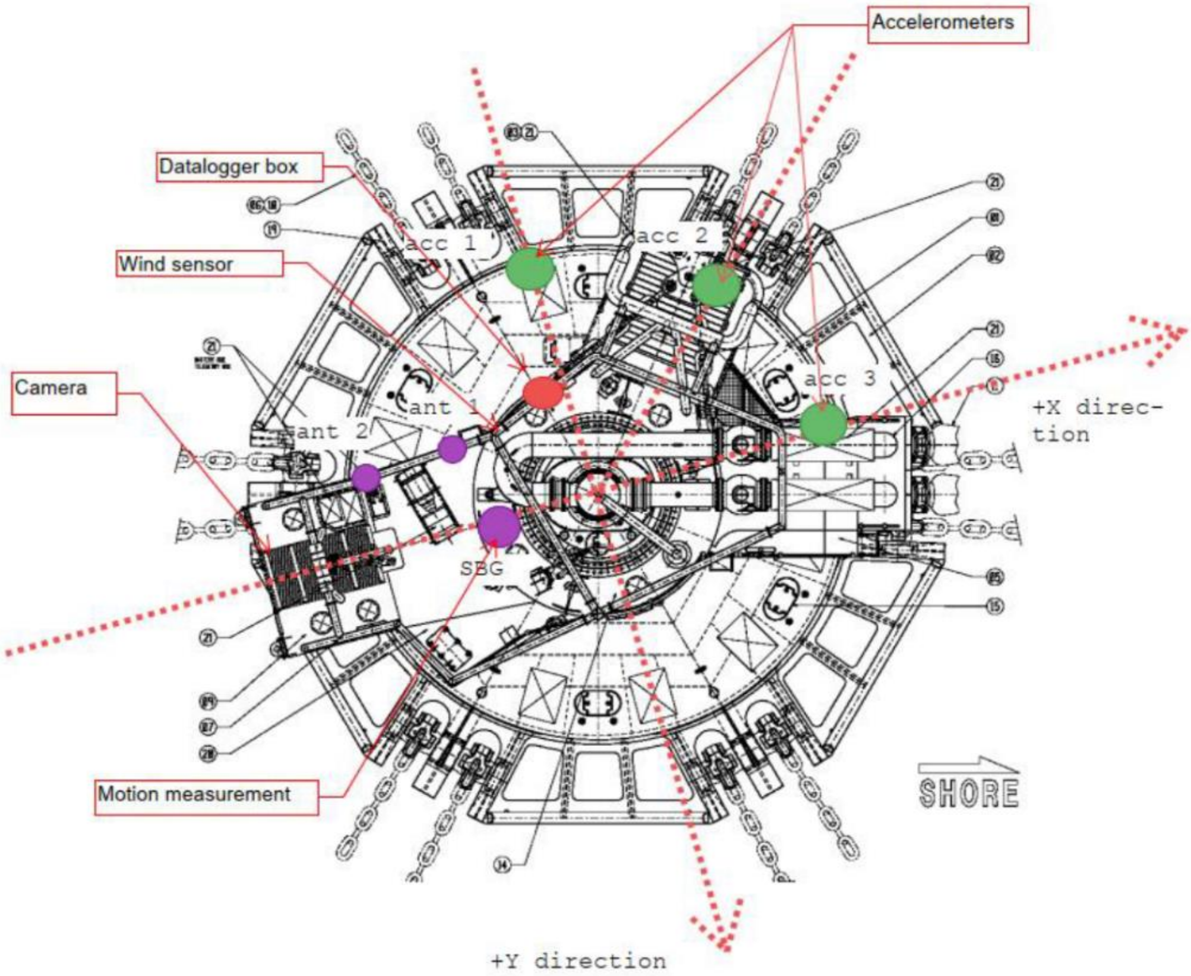

Figure 2-1. Overview of external data instrumentation. Coastal Testbed structure seen from above.

This project has received funding from the European Union's Horizon 2020 research and innovation programme, under the Grant Agreement no. 871571.

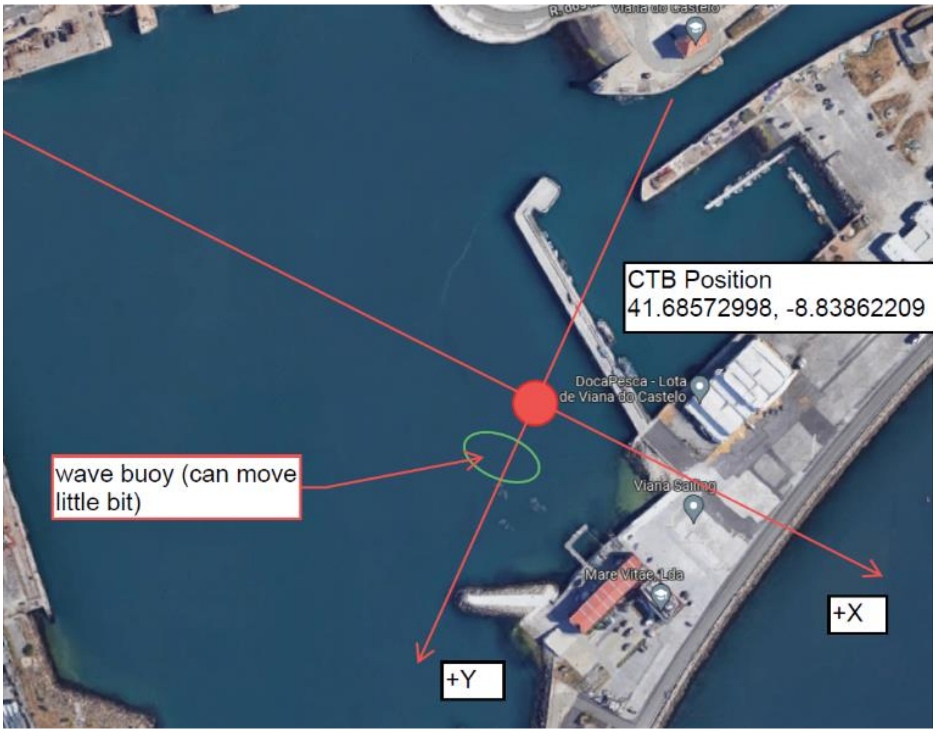

Figure 2-2. Location of the Coastal Testbed structure, the wave buoy and positive X and Y directions.

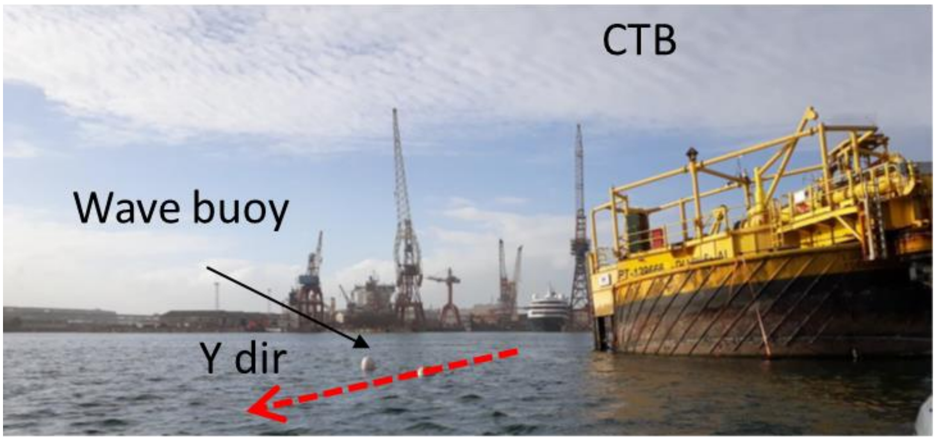

Figure 2-3. Wave buoy next to the Coastal Testbed structure.

All the measurements except the data from the wave buoy were sampled simultaneously with separate DAQ units connected to a PC for data storage and measurement management, including remote access. The wave buoy data were synchronized with the rest of the data offline, based on time stamps. The measurements started in the beginning of September and continued to mid-January 2023. Problems were encountered with motion sensor data that showed inconsistencies and the wind sensor and the wave buoy that were not fully functional throughout the measurement period. However, no critical data was lost. The wave conditions were mostly very calm due to the sheltered harbor location, see Figure 2-4. Waves from passing boats and a severe storm in early January 2023 provided the needed conditions for determining the natural frequency of the structure for the digital twin model.

This project has received funding from the European Union's Horizon 2020 research and innovation programme, under the Grant Agreement no. 871571.

Table 2-1. Motion measurements at the CTB.

Measurement	Location	Name	Unit	Fs [Hz]	Other
Vibration acc * 3	CTB outer circle	1_acc_X, Y, Z	g	200	sensor range +/- 1.5 g
Vibration acc * 3	CTB outer circle	2_acc_X, Y, Z	g	200	sensor range +/- 4 g
Vibration acc * 3	CTB outer circle	2_acc_X, Y, Z	g	200	sensor range +/- 12 g
Vibration acc * 3	CTB inner circle	SBG_ACCEL_X, Y, Z	m/s2	100	
Velocity	CTB inner circle	SBG_GPS_VEL_DOWN	m/s	10	
Inclination * 3	CTB inner circle	SBG_PITCH, ROLL, YAW	Deg	10	
Inclination velocity *3	CTB inner circle	SBG_ROT_X, Y, Z	Deg/s	10	
Motion * 3	CTB inner circle	SBG_SHIPMOTION_HEAVE, SURGE, SWAY	m	10	
Motion velocity * 3	CTB inner circle	SBG_SHIPMOTION_VEL_X, Y, Z	m/s	10	
Yaw angle	CTB inner circle	SBG_TRUE_HEADING_GPS	Deg	10	

Table 2-2. Wind and wave measurements at the CTB.

Measurement	Location	Name	Unit	Fs [Hz]	Other
Wind direction	CTB outer circle	wind_direction	Deg	10	360/0 degrees points North
Wind frequency	CTB outer circle	wind_freq	Hz	10	
Wind speed	CTB outer circle	wind_speed_mps	m/s	10	
Wave buoy movement	At sea about 2 m from CTB	wave_buoy_heave, _north, _west	cm	1.28	Own anchor to the sea bottom

This project has received funding from the European Union's Horizon 2020 research and innovation programme, under the Grant Agreement no. 871571.

Figure 2-4. Example image from web video stream for wave and status monitoring from 24th of January 2023.

2.1.2. Wave and motion response data

Figure 2-5 presents an example of the obtained wave and motion response data from the ATLANTIS Coastal Testbed. Figure 2-6 shows the difference in motion for calm and stormy weather. These time series together with the obtained natural frequency (Figure 2-7) of the floating structure were used for the set-up of the digital twin model and the subsequent predictive maintenance analytics.

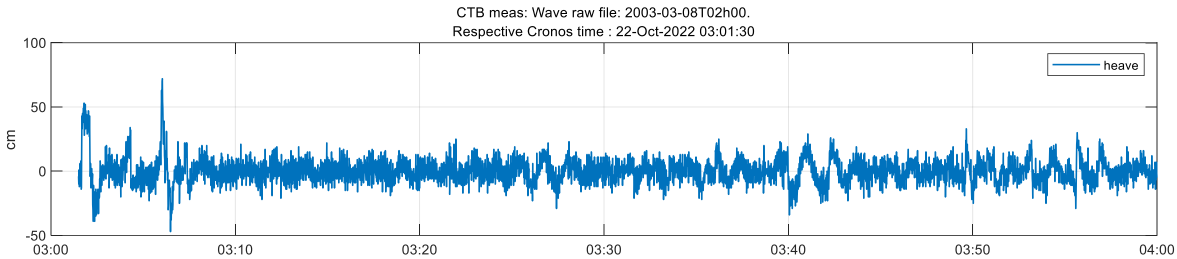

a)

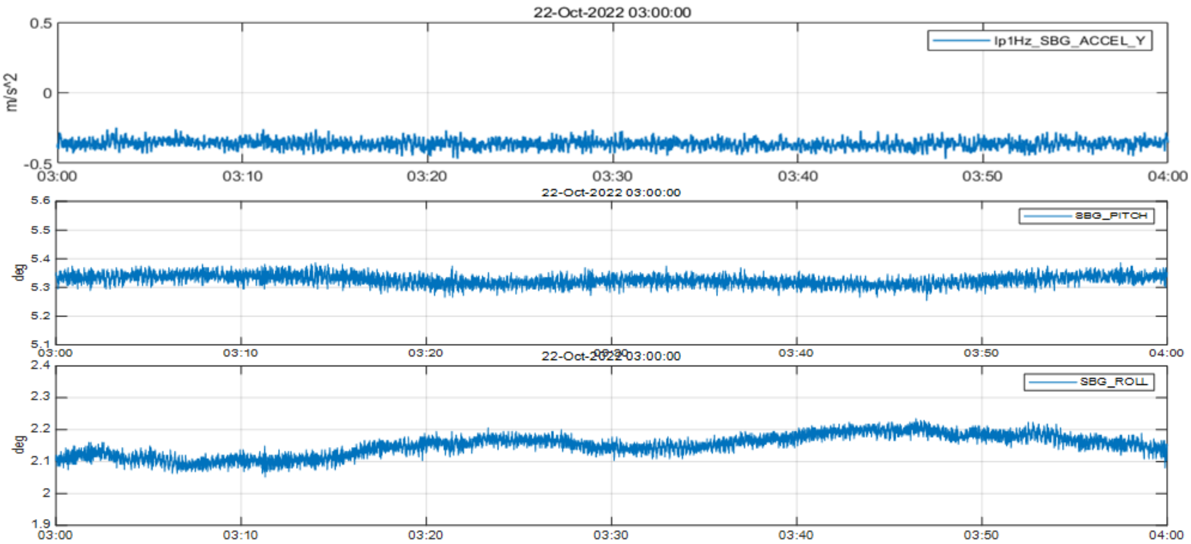

b)

Figure 2-5. An example of a) measured wave excitation (heave) and b) responses in terms of lateral vibration acceleration in Y direction and pitch and roll motions.

This project has received funding from the European Union's Horizon 2020 research and innovation programme, under the Grant Agreement no. 871571.

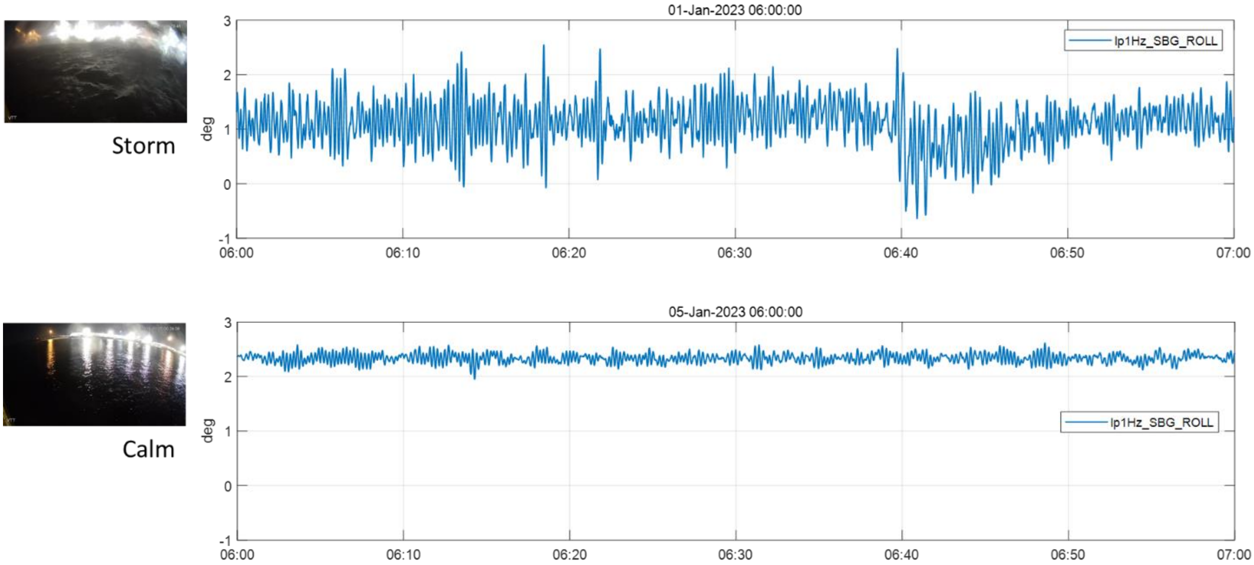

Figure 2-6. Roll response during storm and calm weather.

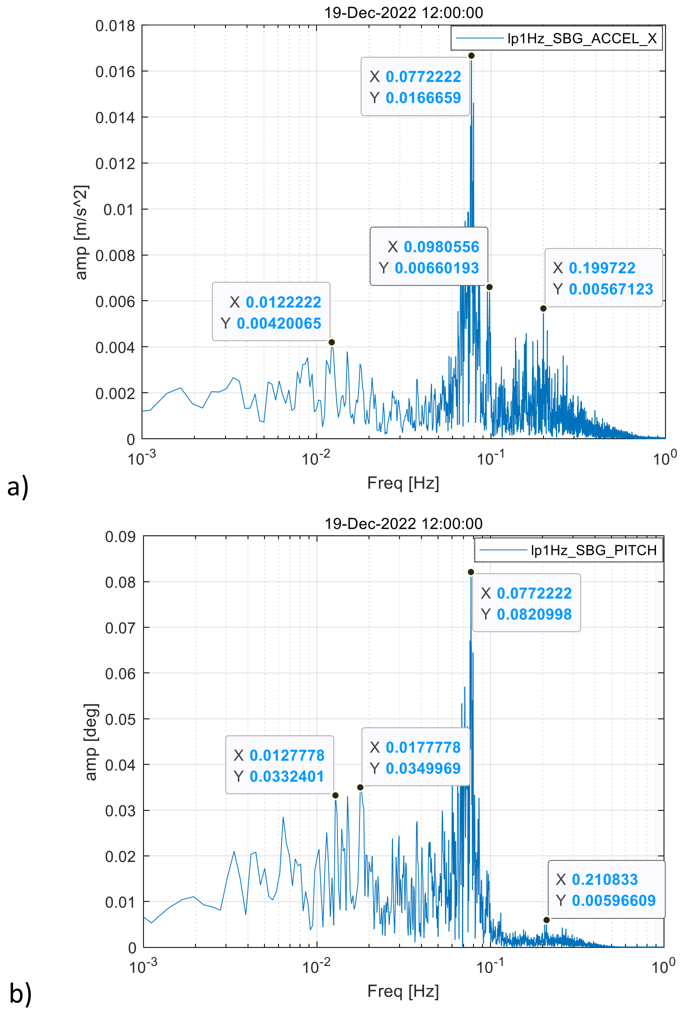

Figure 2-7. Natural mode of the structure – approximately 0.07 Hz – seen from a) Y accelerations and b) pitch motion in frequency domain.

This project has received funding from the European Union's Horizon 2020 research and innovation programme, under the Grant Agreement no. 871571.

2.2. Modelling the floating structure with ANSYS®

2.2.1. Model features

The analysis employed ANSYS® Aqwa, utilized for conducting frequency and time domain simulations to evaluate hydrodynamic behavior, motions, and accelerations, including hydrodynamic and mooring line loads.

A CAD Model (Figure 2-8) was built to be used during simulations, with the origin of the reference axis located in the center of the main cylinder, at the same height as the waterline. The fully loaded draft was considered, and mass properties along with hydrostatics were verified based on the as-built documentation from the real structure. Table 2-3 shows the results for the model and Table 2-4 the adopted radii of gyration.

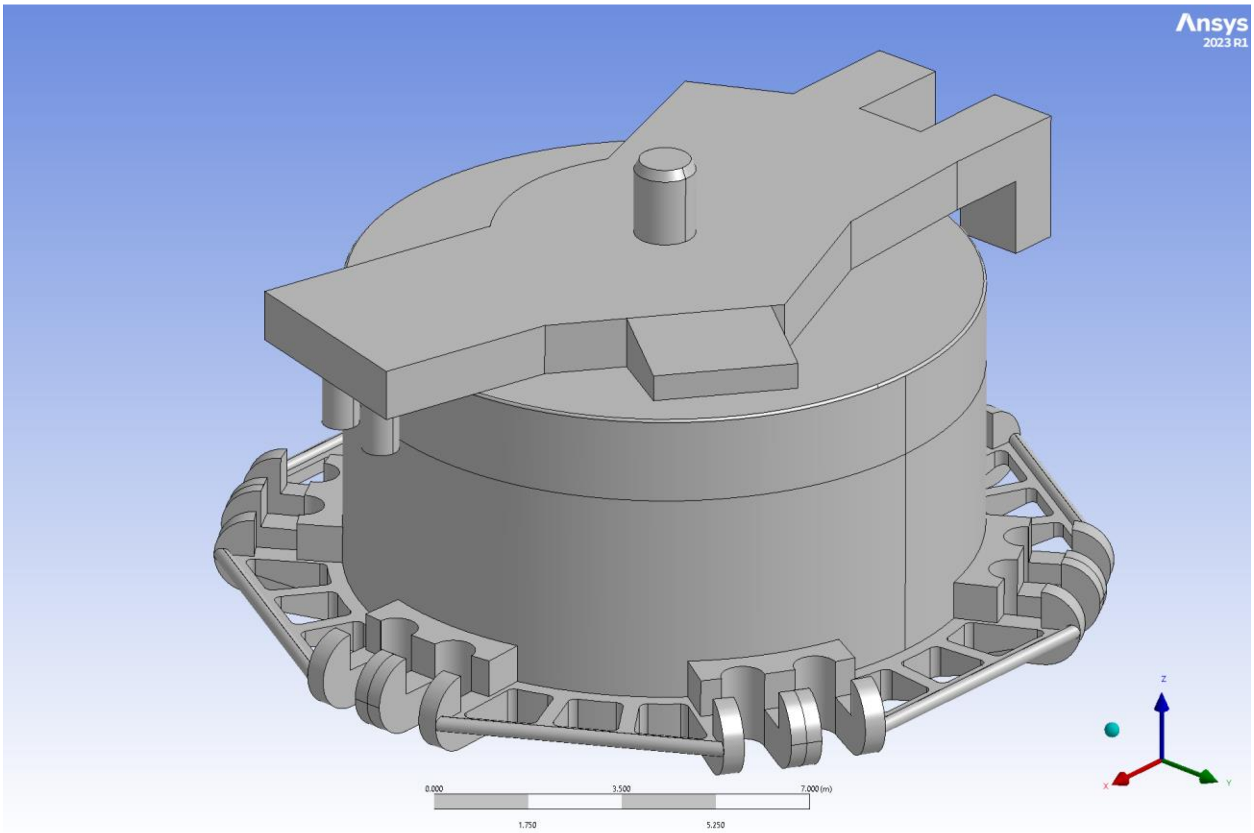

Figure 2-8. Geometry Model

This project has received funding from the European Union's Horizon 2020 research and innovation programme, under the Grant Agreement no. 871571.

Viscous effects play a significant role in evaluating the hydrodynamic behavior of the structure and must be taken into account to ensure that the model is not underdamped. To represent this influence, simplified additional damping coefficients were incorporated for heave, roll, and pitch motions (Table 2-5).

Table 2-3. Main dimensions and Hydrostatics - model and as-built.

		Model	As-built	Discrepancy
Diameter - Main cylinder	m	12.0	12.0	0 %
Height	m	6.5	6.5	0 %
Draft	m	4.83	4.83	0 %
Displacement	m3	586.3	557.5	5 %
KG	m	2.727	2.725	0 %
KB	m	2.294	2.383	-4 %
ZG	m	-2.103	-2.103	0 %
ZB	m	-2.536	-2.445	4 %
AWP	m2	113.1	113.1	0 %
GM	m	1.302	1.483	-12 %
BM	m	1.736	1.825	-5 %

Table 2-4. Radius of gyration.

Radius of gyration		
Kxx	m	3.720
Kyy	m	3.916
Kzz	m	4.434

Table 2-5. Additional Viscous Damping Coefficients

Additional Damping B_{visc}/B_{crit}	
Heave	8 %
Roll	11 %
Pitch	11 %

2.2.1. Set-up of load cases

2.2.1.1. Mooring Lines

To simulate scenarios as similar as possible to real operations, it is assumed that the structure is installed with a catenary mooring system, which includes 3 lines with a 120° angle between each of them (Figure 2-9). This system is composed of two sections, with chains in the lower part touching the seabed, and a polyester line in the upper part. The mechanical properties of the mooring lines were based on (Azcona & Vittori, 2019) and are presented in Tables 2-6 to 2-8.

This project has received funding from the European Union's Horizon 2020 research and innovation programme, under the Grant Agreement no. 871571.

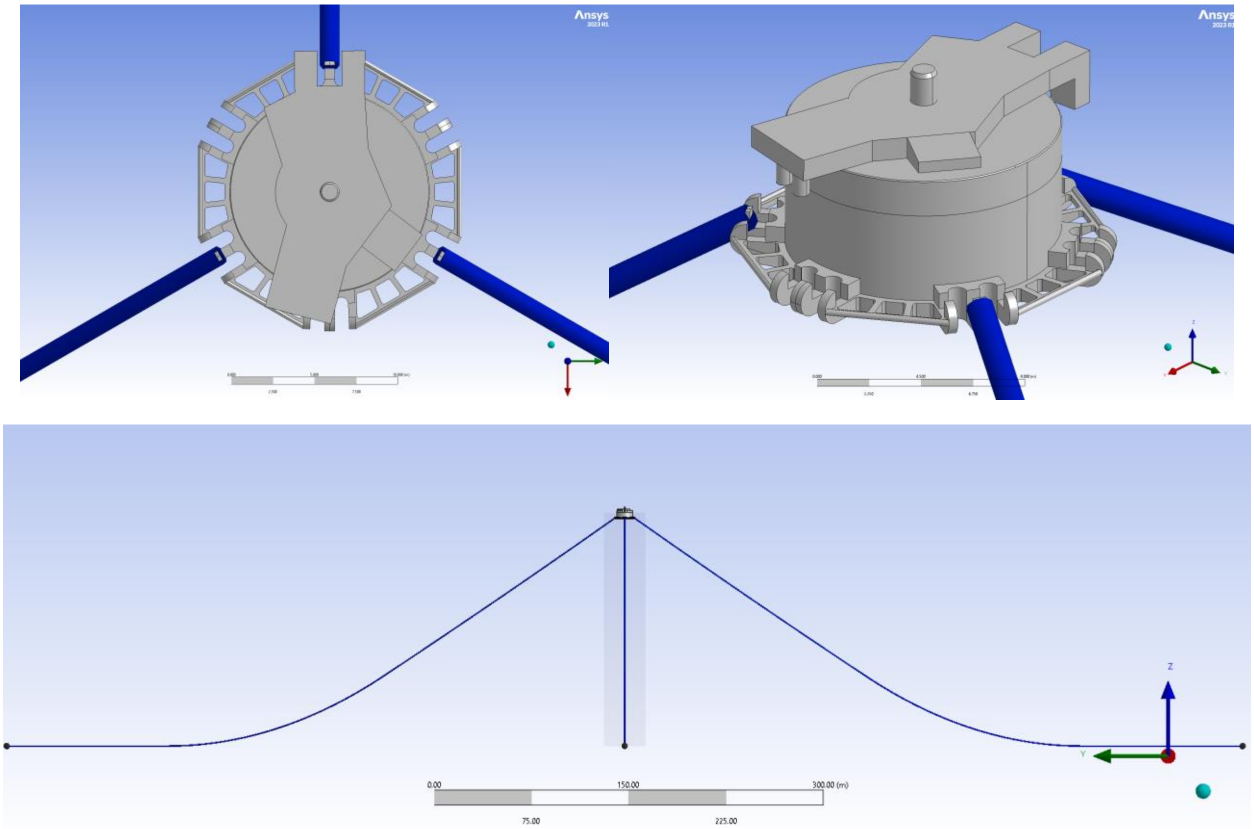

Figure 2-9. Mooring lines modelled in ANSYS® Aqwa.

Table 2-6. Mooring line properties - (Azcona & Vittori, 2019).

	Mooring Lines				
	Length (m)	Mass/Unit Length (kg/m)	Cross-sec. Area (m2) (m2)	Stiffness EA (N)	Diameter (m)
Chain	344	200	0.08245	2.80E+09	0.324
Polyester	239	24.5	0.01791	4.32E+06	0.151

Table 2-7. Mooring attachment points at the structure and seabed - ANSYS® modelling.

		Attachment points		
		x	y	z
Structure 1	m	3.86	6.59	-3.7
Structure 2	m	-7.55	0.0	-3.7
Structure 3	m	3.86	-6.59	-3.7
Ground 1	m	550.0	476.31	-180.0
Ground 2	m	-275.0	0.0	-180.0
Ground 3	m	-275.0	-476.31	-180.0

This project has received funding from the European Union's Horizon 2020 research and innovation programme, under the Grant Agreement no. 871571.

Table 2-8. Mooring lines in calm waters - ANSYS® Aqwa Results.

Cables Initial Condition		
Distance between attachment points	m	570.3
Initial Cable Tension at Seabed	N	3.98E+05
Initial Cable Tension at Structure	N	4.66E+05

2.2.1.2. Environmental Conditions

It is assumed that the structure will operate along Portugal´s coast with water depth of 180 meters. Therefore, the wave scatter diagram provided by (British Maritime Technology, 1986) for the Marsden Area 16 (see Figure 2-10) is employed to define the conditions for simulation.

This diagram provides the occurrence of various combinations of wave heights (Hs) and peak periods (Tp). As there is no available data regarding the direction of the waves, it is assumed that the occurrence is the same regardless of the direction. In the specified area, wave heights range up to 11.5 meters, with periods ranging from 4.5 to 12.5 seconds.

Additionally, considering the symmetry of the model, wave directions ranging from 0 degrees (direction of +x) to 90 degrees (direction of +y) were simulated. Table 2-9 shows all the values combined to define wave conditions, including 6 wave directions, 11 wave heights and 9 peak periods, thereby yielding a total of 594 distinct combinations of wave conditions.

Table 2-9. Environmental conditions for simulations.

Water Depth	**m**	180
Wave Direction	**degrees**	0, 15, 30, 45, 60, 90
Significant Wave Height (Hs)	**m**	1.5, 2.5, 3.5, 4.5, 5.5, 6.5, 7.5, 8.5, 9.5, 10.5, 11.5
Peak Period (Tp)	**s**	4.5, 5.5, 6.5, 7.5, 8.5, 9.5, 10.5, 11.5, 12
Wave Spectra	**-**	Jonswap

This project has received funding from the European Union's Horizon 2020 research and innovation programme, under the Grant Agreement no. 871571.

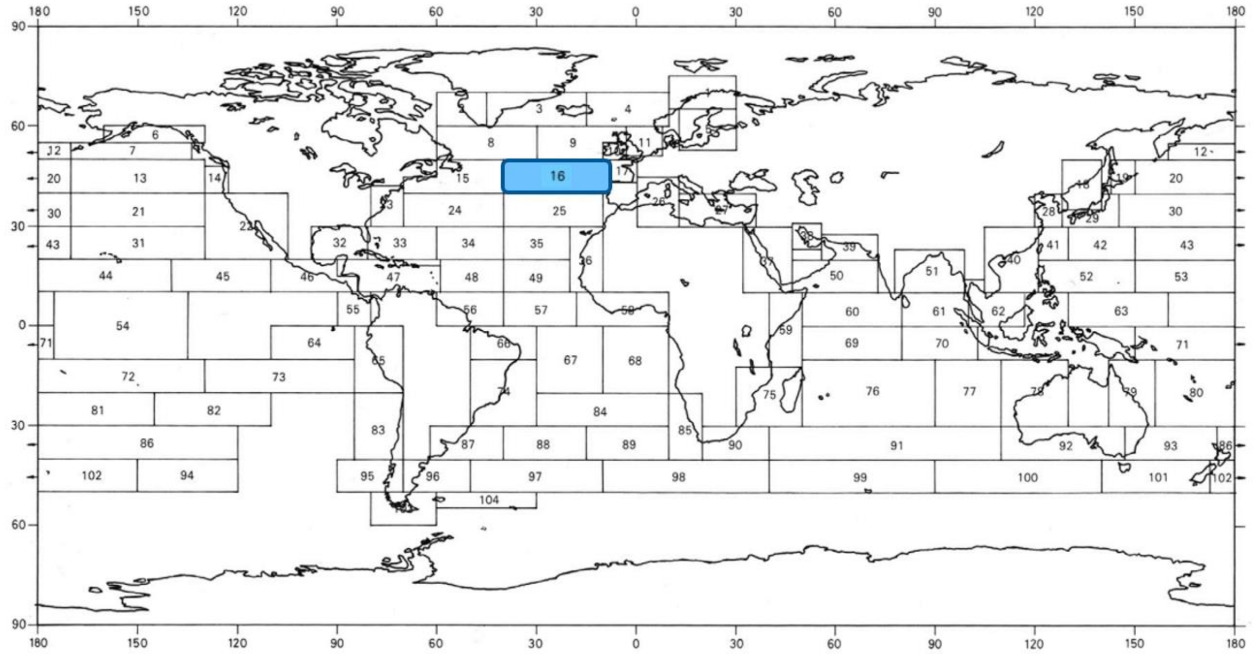

Figure 2-10. Marsden Area 16 (British Maritime Technology, 1986).

This project has received funding from the European Union's Horizon 2020 research and innovation programme, under the Grant Agreement no. 871571.

3. Predictive maintenance with O&M module

3.1. Operational limits

There are multiple and different operation criteria for human based marine operations. One simplified approach is presented in reference (Nordforsk, 1987). It represents limiting motion criteria for vibration acceleration RMS and roll RMS values, and different work types: light manual work, heavy manual work, intellectual work, etc. Here the following operational criteria were adopted according to the limits for heavy manual work (Table 3-1).

A point located outside the gravity center was taken to analyze the motions. Considering inspection operations, a location close to the mooring lines was considered (Figure 3-1) and has the following coordinates shown in Table 3-2.

By combining the various wave directions, significant heights, and peak periods shown in Table 2-10, a total of 594 simulations in the frequency domain were conducted. The results are plotted along with the operational limit curve for each criterion, see Figures 3-2 and 3-3.

Table 3-1. Operational limits criteria.

	Criteria	Limit
1	RMS Roll – Rx	4 deg
2	RMS Pitch - Ry	4 deg
3	RMS Lateral Acceleration - X	0.07g
4	RMS Lateral Acceleration - Y	0.07g
5	RMS Vertical Acceleration - Z	0.15g

Table 3-2. Reference point in the structure to used during motions analysis.

Inspection Point		
x (m)	**y(m)**	**z(m)**
-6.0	0.0	-4.0

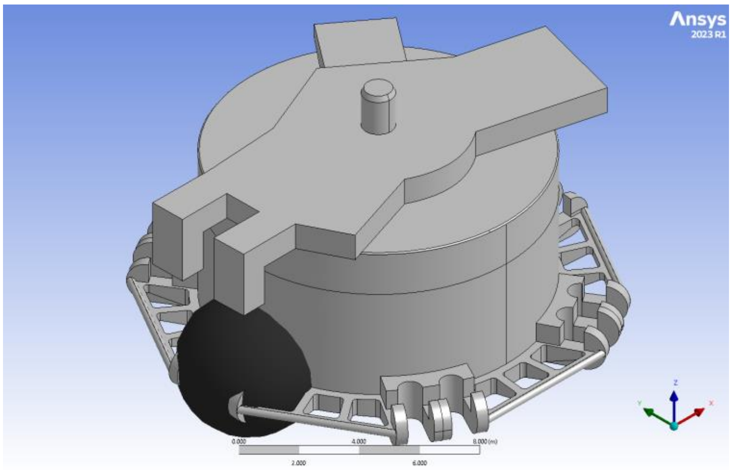

Figure 3-1. Reference point for motion analysis (darkened area).

This project has received funding from the European Union's Horizon 2020 research and innovation programme, under the Grant Agreement no. 871571.

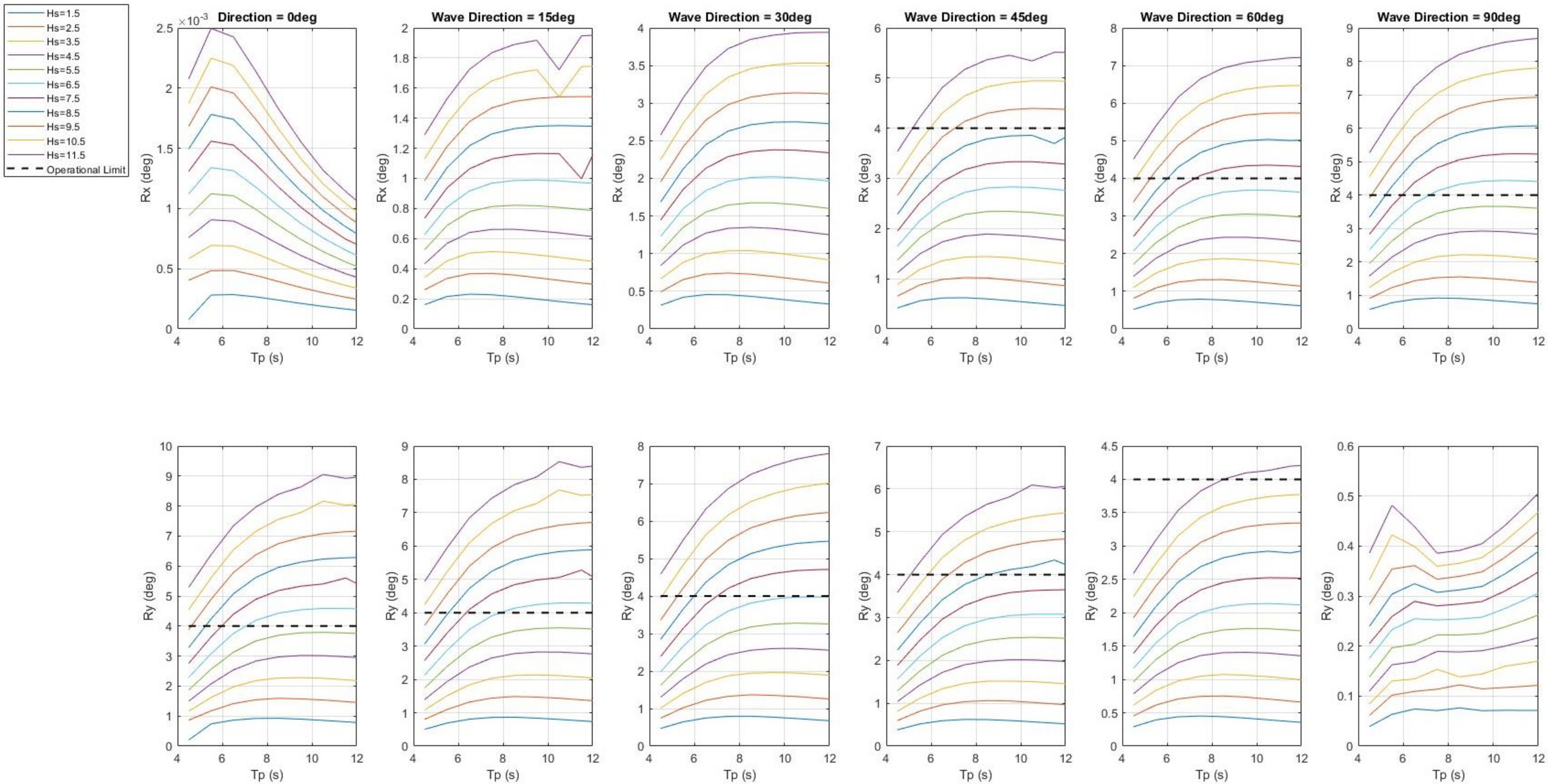

Figure 3-2. Simulated roll (Rx) and pitch (Ry) for different wave heights (Hs) and directions as a function of peak period (Tp) in comparison to operational limit criterion of 4 degrees roll or pitch motion.

This project has received funding from the European Union's Horizon 2020 research and innovation programme, under the Grant Agreement no. 871571.

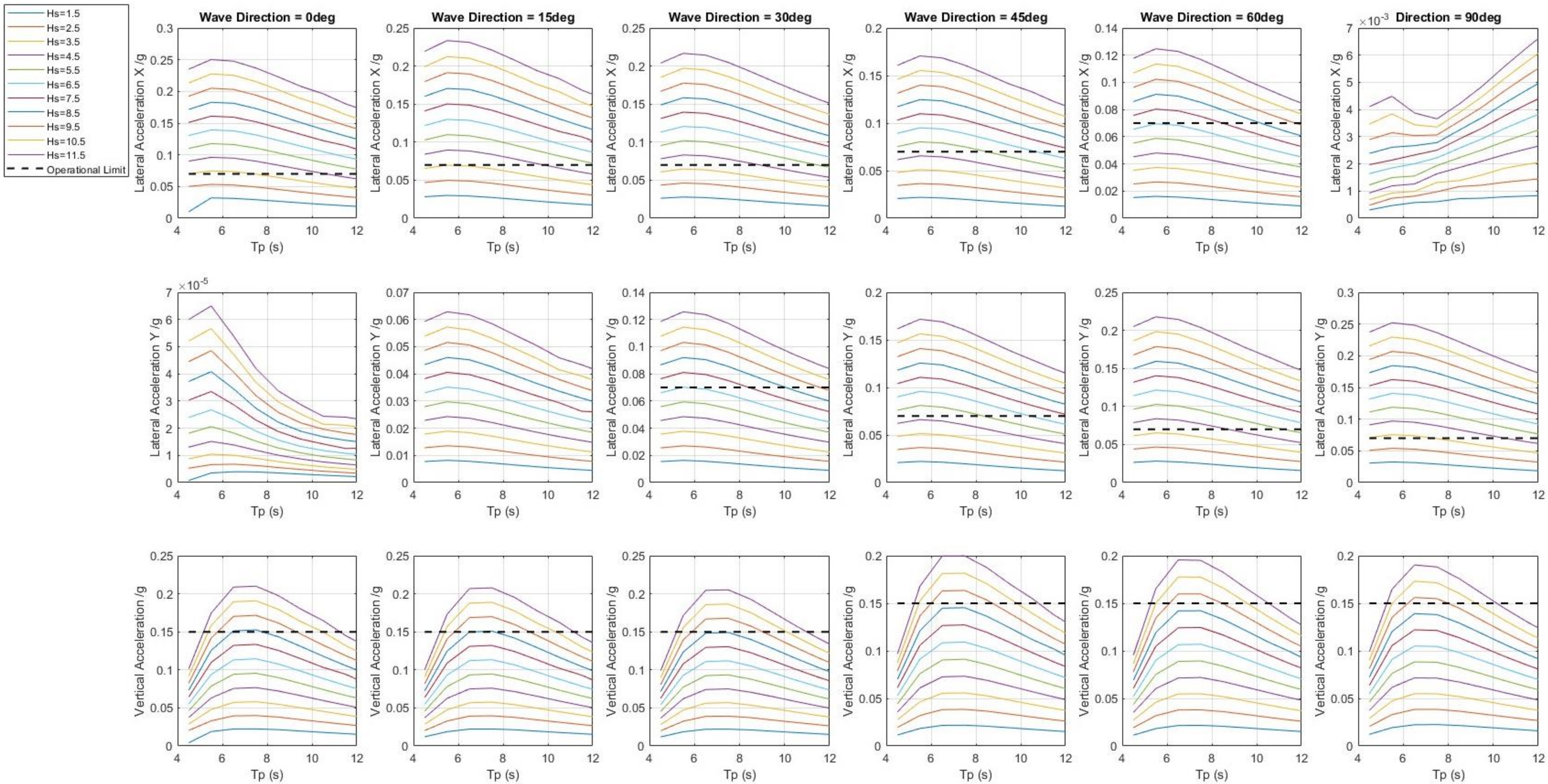

Figure 3-3. Simulated lateral (X and Y) and vertical accelerations for different wave heights (Hs) and directions as a function of peak period (Tp) in comparison to operational limit criterion of 0.07 g for lateral accelerations and 0.15 g for vertical acceleration.

This project has received funding from the European Union's Horizon 2020 research and innovation programme, under the Grant Agreement no. 871571.

3.1.1. Limiting significant wave height

Utilizing the criteria outlined in Table 3-1, a limiting wave height can be defined as the maximum wave height that complies with the criteria for each combination of wave direction and peak period. Table 3-3 shows the limiting significant wave heights for the five operational limit criteria: roll, pitch, and lateral and vertical accelerations. Most limiting wave height is indicated in red and least limiting wave height in green.

Based on the results, the most restrictive criterion is the lateral accelerations, which can be as low as 2.5 meters for shorter peak periods ranging from 4.5 to 6.5 seconds. Conversely, the least stringent criterion pertains to vertical acceleration, with minimum limiting Hs values of 7.5 meters for Tp between 6.5 and 7.5 seconds. When considering the combined criteria, the limiting Hs varies between 2.5 and 6.5 meters, varying with the wave direction and peak period. The combined criteria give the lowest i.e. the limiting wave height for each combination of peak period and wave direction. Here this equals a combination of lateral accelerations criteria (X and Y).

Table 3-3. Limiting significant wave height. Most limiting wave height is indicated in red and least limiting wave height in green.

	Limit Hs - Criteria 1: RMS Roll ≤ 4 degrees					
Dir. / Tp	0 deg	15 deg	30 deg	45 deg	60 deg	90 deg
4.5s	11.5m	11.5m	11.5m	11.5m	10.5m	9.5m
5.5s	11.5m	11.5m	11.5m	10.5m	8.5m	7.5m
6.5s	11.5m	11.5m	11.5m	9.5m	7.5m	6.5m
7.5s	11.5m	11.5m	11.5m	8.5m	6.5m	5.5m
8.5s	11.5m	11.5m	11.5m	8.5m	6.5m	5.5m
9.5s	11.5m	11.5m	11.5m	8.5m	6.5m	5.5m
10.5	11.5m	11.5m	11.5m	8.5m	6.5m	5.5m
11.5	11.5m	11.5m	11.5m	8.5m	6.5m	5.5m
12s	11.5m	11.5m	11.5m	8.5m	6.5m	5.5m

	Limit Hs - Criteria 2: RMS Pitch ≤ 4 degrees					
Dir. / Tp	0 deg	15 deg	30 deg	45 deg	60 deg	90 deg
4.5s	9.5m	9.5m	10.5m	11.5m	11.5m	11.5m
5.5s	7.5m	8.5m	8.5m	10.5m	11.5m	11.5m
6.5s	6.5m	6.5m	7.5m	9.5m	11.5m	11.5m
7.5s	5.5m	6.5m	6.5m	8.5m	11.5m	11.5m
8.5s	5.5m	5.5m	6.5m	8.5m	10.5m	11.5m
9.5s	5.5m	5.5m	6.5m	7.5m	10.5m	11.5m
10.5	5.5m	5.5m	6.5m	7.5m	10.5m	11.5m
11.5	5.5m	5.5m	6.5m	7.5m	10.5m	11.5m
12s	5.5m	5.5m	6.5m	7.5m	10.5m	11.5m

	Limit Hs - Criteria 3: RMS X acceleration ≤ 0.07g					
Dir. / Tp	0 deg	15 deg	30 deg	45 deg	60 deg	90 deg
4.5s	2.5m	3.5m	3.5m	4.5m	6.5m	11.5m
5.5s	2.5m	3.5m	3.5m	4.5m	6.5m	11.5m
6.5s	2.5m	3.5m	3.5m	4.5m	6.5m	11.5m
7.5s	3.5m	3.5m	3.5m	4.5m	6.5m	11.5m
8.5s	3.5m	3.5m	3.5m	5.5m	7.5m	11.5m
9.5s	3.5m	3.5m	4.5m	5.5m	7.5m	11.5m
10.5	3.5m	4.5m	4.5m	5.5m	8.5m	11.5m
11.5	4.5m	4.5m	5.5m	6.5m	8.5m	11.5m
12s	4.5m	4.5m	5.5m	6.5m	9.5m	11.5m

	Limit Hs - Criteria 4: RMS Y acceleration ≤ 0.07g					
Dir. / Tp	0 deg	15 deg	30 deg	45 deg	60 deg	90 deg
4.5s	11.5m	11.5m	6.5m	4.5m	3.5m	2.5m
5.5s	11.5m	11.5m	5.5m	4.5m	3.5m	2.5m
6.5s	11.5m	11.5m	6.5m	4.5m	3.5m	2.5m
7.5s	11.5m	11.5m	6.5m	4.5m	3.5m	3.5m
8.5s	11.5m	11.5m	7.5m	5.5m	3.5m	3.5m
9.5s	11.5m	11.5m	7.5m	5.5m	4.5m	3.5m
10.5	11.5m	11.5m	8.5m	6.5m	4.5m	3.5m
11.5	11.5m	11.5m	8.5m	6.5m	5.5m	4.5m
12s	11.5m	11.5m	9.5m	6.5m	5.5m	4.5m

	Limit Hs - Criteria 5: RMS Z acceleration ≤ 0.15g					
Dir. / Tp	0 deg	15 deg	30 deg	45 deg	60 deg	90 deg
4.5s	11.5m	11.5m	11.5m	11.5m	11.5m	11.5m
5.5s	9.5m	9.5m	9.5m	9.5m	9.5m	10.5m
6.5s	7.5m	8.5m	8.5m	8.5m	8.5m	8.5m
7.5s	7.5m	7.5m	8.5m	8.5m	8.5m	8.5m
8.5s	8.5m	8.5m	8.5m	8.5m	9.5m	9.5m
9.5s	9.5m	9.5m	9.5m	9.5m	9.5m	10.5m
10.5	10.5m	10.5m	10.5m	10.5m	10.5m	11.5m
11.5	11.5m	11.5m	11.5m	11.5m	11.5m	11.5m
12s	11.5m	11.5m	11.5m	11.5m	11.5m	11.5m

	Limit Hs - Combined criteria					
Dir. / Tp	0 deg	15 deg	30 deg	45 deg	60 deg	90 deg
4.5s	2.5m	3.5m	3.5m	4.5m	3.5m	2.5m
5.5s	2.5m	3.5m	3.5m	4.5m	3.5m	2.5m
6.5s	2.5m	3.5m	3.5m	4.5m	3.5m	2.5m
7.5s	3.5m	3.5m	3.5m	4.5m	3.5m	3.5m
8.5s	3.5m	3.5m	3.5m	5.5m	3.5m	3.5m
9.5s	3.5m	3.5m	4.5m	5.5m	4.5m	3.5m
10.5	3.5m	4.5m	4.5m	5.5m	4.5m	3.5m
11.5	4.5m	4.5m	5.5m	6.5m	5.5m	4.5m
12s	4.5m	4.5m	5.5m	6.5m	5.5m	4.5m

This project has received funding from the European Union's Horizon 2020 research and innovation programme, under the Grant Agreement no. 871571.

3.1.2. Region based downtime assessment

Defining the maximum wave height that complies with the criteria is important. However, for a better planning and scheduling of maintenance operations, the probability of occurrence for each wave condition in the location where the structure will operate needs to be considered.

To evaluate the potential durations of the restrictions due weather conditions for these operations, downtime can be calculated using the wave scatter diagram of the region. This calculation should incorporate the probability of exceedance of limiting Hs for each period:

$$Downtime\ (Hs_{limiting}, Tp) = \sum p\ (Hs \geq Hs_{limiting}\ , Tp) \qquad [1]$$

The downtime corresponding to the criteria is outlined below. Table 3-4 shows that while lateral accelerations in waves at 0 and 90 degrees and Tp of 4.5, 5.5 and 6.5 seconds resulted in lower limiting Hs (Table 3-3), these conditions are not the most likely to cause downtime (maximum probability of 5%).

Table 3-4. Downtime based on operational limits and regional wave scatter diagram.

	Downtime - Criteria 1: RMS Roll ≤ 4 degrees					
Tp \ Dir.	0 deg	15 deg	30 deg	45 deg	60 deg	90 deg
4.5s	0.0%	0.0%	0.0%	0.0%	0.0%	0.0%
5.5s	0.0%	0.0%	0.0%	0.0%	0.0%	0.0%
6.5s	0.0%	0.0%	0.0%	0.0%	0.0%	0.1%
7.5s	0.0%	0.0%	0.0%	0.1%	0.5%	1.4%
8.5s	0.0%	0.0%	0.0%	0.3%	1.6%	3.5%
9.5s	0.0%	0.0%	0.0%	0.6%	2.3%	4.3%
10.5	0.1%	0.1%	0.1%	0.6%	1.9%	3.2%
11.5	0.0%	0.0%	0.0%	0.4%	1.1%	1.7%
12s	0.0%	0.0%	0.0%	0.1%	0.3%	0.5%

	Downtime - Criteria 2: RMS Pitch ≤ 4 degrees					
Tp \ Dir.	0 deg	15 deg	30 deg	45 deg	60 deg	90 deg
4.5s	0.0%	0.0%	0.0%	0.0%	0.0%	0.0%
5.5s	0.0%	0.0%	0.0%	0.0%	0.0%	0.0%
6.5s	0.1%	0.1%	0.0%	0.0%	0.0%	0.0%
7.5s	1.4%	0.5%	0.5%	0.1%	0.0%	0.0%
8.5s	3.5%	3.5%	1.6%	0.3%	0.0%	0.0%
9.5s	4.3%	4.3%	2.3%	1.2%	0.1%	0.0%
10.5	3.2%	3.2%	1.9%	1.1%	0.2%	0.1%
11.5	1.7%	1.7%	1.1%	0.7%	0.1%	0.0%
12s	0.5%	0.5%	0.3%	0.2%	0.0%	0.0%

	Downtime - Criteria 3: RMS X acceleration ≤ 0.07g					
Tp \ Dir.	0 deg	15 deg	30 deg	45 deg	60 deg	90 deg
4.5s	0.0%	0.0%	0.0%	0.0%	0.0%	0.0%
5.5s	0.5%	0.1%	0.1%	0.0%	0.0%	0.0%
6.5s	5.0%	1.9%	1.9%	0.6%	0.1%	0.0%
7.5s	8.0%	8.0%	8.0%	3.5%	0.5%	0.0%
8.5s	13.6%	13.6%	13.6%	3.5%	0.7%	0.0%
9.5s	12.4%	12.4%	7.7%	4.3%	1.2%	0.0%
10.5	7.1%	5.0%	5.0%	3.2%	0.6%	0.1%
11.5	2.4%	2.4%	1.7%	1.1%	0.4%	0.0%
12s	0.7%	0.7%	0.5%	0.3%	0.0%	0.0%

	Downtime - Criteria 4: RMS Y acceleration ≤ 0.07g					
Tp \ Dir.	0 deg	15 deg	30 deg	45 deg	60 deg	90 deg
4.5s	0.0%	0.0%	0.0%	0.0%	0.0%	0.0%
5.5s	0.0%	0.0%	0.0%	0.0%	0.1%	0.5%
6.5s	0.0%	0.0%	0.1%	0.6%	1.9%	5.0%
7.5s	0.0%	0.0%	0.5%	3.5%	8.0%	8.0%
8.5s	0.0%	0.0%	0.7%	3.5%	13.6%	13.6%
9.5s	0.0%	0.0%	1.2%	4.3%	7.7%	12.4%
10.5	0.1%	0.1%	0.6%	1.9%	5.0%	7.1%
11.5	0.0%	0.0%	0.4%	1.1%	1.7%	2.4%
12s	0.0%	0.0%	0.0%	0.3%	0.5%	0.7%

	Downtime - Criteria 5: RMS Z acceleration ≤ 0.15g					
Tp \ Dir.	0 deg	15 deg	30 deg	45 deg	60 deg	90 deg
4.5s	0.0%	0.0%	0.0%	0.0%	0.0%	0.0%
5.5s	0.0%	0.0%	0.0%	0.0%	0.0%	0.0%
6.5s	0.0%	0.0%	0.0%	0.0%	0.0%	0.0%
7.5s	0.2%	0.2%	0.1%	0.1%	0.1%	0.1%
8.5s	0.3%	0.3%	0.3%	0.3%	0.1%	0.1%
9.5s	0.3%	0.3%	0.3%	0.3%	0.3%	0.1%
10.5	0.2%	0.2%	0.2%	0.2%	0.2%	0.1%
11.5	0.0%	0.0%	0.0%	0.0%	0.0%	0.0%
12s	0.0%	0.0%	0.0%	0.0%	0.0%	0.0%

	Downtime - Combined criteria					
Tp \ Dir.	0 deg	15 deg	30 deg	45 deg	60 deg	90 deg
4.5s	0.0%	0.0%	0.0%	0.0%	0.0%	0.0%
5.5s	0.5%	0.1%	0.1%	0.0%	0.1%	0.5%
6.5s	5.0%	1.9%	1.9%	0.6%	1.9%	5.0%
7.5s	8.0%	8.0%	8.0%	3.5%	8.0%	8.0%
8.5s	13.6%	13.6%	13.6%	3.5%	13.6%	13.6%
9.5s	12.4%	12.4%	7.7%	4.3%	7.7%	12.4%
10.5	7.1%	5.0%	5.0%	3.2%	5.0%	7.1%
11.5	2.4%	2.4%	1.7%	1.1%	1.7%	2.4%
12s	0.7%	0.7%	0.5%	0.3%	0.5%	0.7%

This project has received funding from the European Union's Horizon 2020 research and innovation programme, under the Grant Agreement no. 871571.

When the occurrence of local waves is taken into account, the critical conditions entail higher periods, ranging between 7.5 and 9.5 seconds, leading to a downtime probability reaching up to 13.6%. As for vertical acceleration, it remains the least critical criterion, with a maximum probability of 0.3% for causing downtime.

3.1.3. Operation based downtime assessment

In the previous chapter, the downtime was evaluated statistically based on expected wave heights for the region. However, at each region, and at every spot within the regional area, operational burden varies. Variation is based on the materialized weather and wave conditions at these specific spots. Thus, the sea state, and operational and loadings conditions are not equal even within one area. It is important to monitor these emerged conditions locally e.g. at each floating wind power production unit. The key is data. E.g. vibration acceleration, inclination, and loading measurements over different segments and locations of these production units could be utilized, and produced to information with further purposes both for unit wise purposes and for benchmarking purposes with other units.

Here the data was generated with the virtual model, and composed to time series containing variating segment lengths from selected set of circumstances. These composed data sets mimic the variating responses at the modelled CTB unit over selected time frame both for shorter, e.g. day wise, or year wise analysis. The cases which were utilized for individual data composition are presented in Table 3-5.

Table 3-5. Simulated data sources used for the data composition.

Case #	Occurrence [%]	Wave direction [deg]	Peak period Tp [s]	Wave high Hs [m]
0	Minor (extreme)	0	12	11,5
1	6.4	0	8,5	3,5
2	8	0	8,5	2,5
3	7,8	45	7,5	1,5
4	5,3	45	6,5	1,5
5	5,1	45	8,5	1,5
6	2,2	45	6,5	0,5

Each of the simulation case contains 3 hours of data sampled with a one second time interval. In each case there 16 simulated responses are recorded of which vibration acceleration, loading and rotation responses are utilized. These responses and their locations are presented in Table 3-6.

Table 3-6. Simulated responses at the selected mooring line inspection point on the virtual CTB.

Responses	Direction	Name	Unit
vibration acceleration	lateral	Acc X	m/s2
vibration acceleration	lateral	Acc Y	m/s2
vibration acceleration	verical	Acc Z	m/s2
Loading	along cable	Cable line A	N
Loading	along cable	Cable line B	N
Loading	along cable	Cable line C	N
Rotation	roll	Angle RX	deg
Rotation	pitch	Angle RY	deg
Rotation	yaw	Angle RZ	deg

This project has received funding from the European Union's Horizon 2020 research and innovation programme, under the Grant Agreement no. 871571.

3.1.3.1. Vibration acceleration-based analysis

In order to demonstrate the materialized weather conditions, the data was first composed to limited segments lasting three hours but containing in random order random share of each (or otherwise selected) case. An example of a composed data case containing three hours of data is presented in Figure 3-4. Between each case there is a 10 min time gap for the purpose of separating the cases.

The same can be done for all the simulated measurements. The purpose here is not to present how the conditions can be quickly composed but to show how these can be utilized e.g. for operational analysis, including i) analysis related to favourable operation conditions for human based maintenance criteria evaluations and ii) maintenance interval evaluations e.g. for robot deployment aligned with the need of the Atlantis project.

The first case will utilize the data presented in Figure 3-4 for the operation criteria analysis. For that purpose, data profiling is used. In profiling, relevant features of the operational history of a unit is logged and analysed. Here a new key characteristic is extracted: time-at-level (TAL). It facilitates the monitoring of current operational state and history in a compact form convenient for maintenance operability analysis.

The time-at-level (TAL) method counts the time spent in different operating regions. However, information about the variability of the profiled variable is not retained, thus it is not suitable for analysis of dynamic effects since the time in each region might be due to static or dynamic responses.

Here, the main objective for using TAL based profiling is to utilize it for evaluating shares of the favorable weather window and for unfavorable weather downtime. Here with **weather window** we mean interval of time during which the environmental conditions allow execution of a specific marine operation, and respectively **weather downtime** intervals of time which the environmental conditions are too severe to allow the execution (61400-3-1:2019-04.). Criteria for these varies based on operation and operator: e.g. the human based maintenance operation criteria are different to robot criteria, etc.

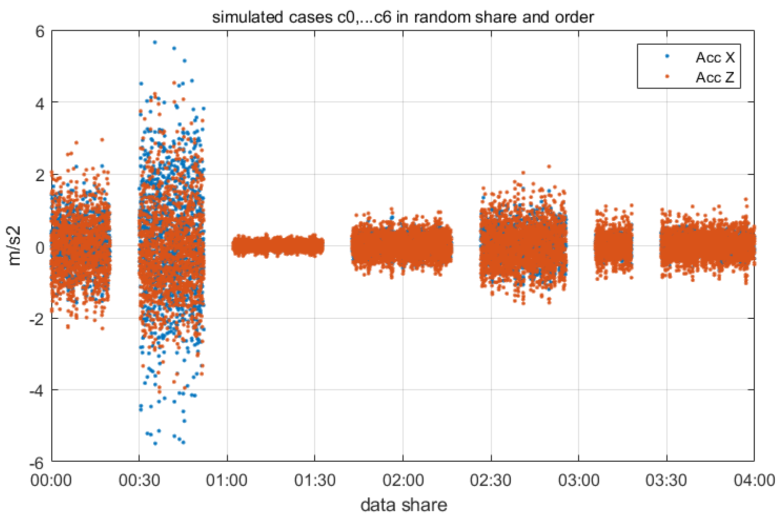

Figure 3-4. Data case representing simulated vibration acceleration in lateral (X) and vertical (Z) direction composed of short duration data segments from cases 0 to 6. The order and share (in percentage) of the cases are: c1 0.11, c0 0.12, c6 0.17, c4 0.19, c2 0.16, c5 0.07 and c3 0.18.

This project has received funding from the European Union's Horizon 2020 research and innovation programme, under the Grant Agreement no. 871571.

As discussed in Chapter 3.1, the limiting operational criterion in its simplest form is RMS value e.g. of vibration acceleration or rotation (see Table 3-1). The simulated data from the virtual model are pure time domain data. Here these are converted to RMS values by using moving RMS filtering:

$$moving\ RMS(i) = \sqrt{\frac{1}{n}\sum_{k=i-n+1}^{i} x^2(k)} \qquad [2]$$

The length of the moving window length n was selected to be 10 s. x in Equation [2] is the raw data. This also reduces the effect of possible data anomalies that are not realistic. Figure 3-5 presents in time domain moving RMS values of Figure 3-4. These RMS values can be used for operation criteria analysis.

For the generation of the TAL profiles the composed 3 h data was first repeated consecutively into a dataset lasting a year (8760 h). In this rehearsal the same data was repeated, but naturally variated datasets could be used, which is what happens in practise in the real world. Figure 3-6 shows TAL values profiled to the example vibration acceleration data (see Figure 3-5) in lateral direction and Figure 3-7 shows the same in vertical direction.

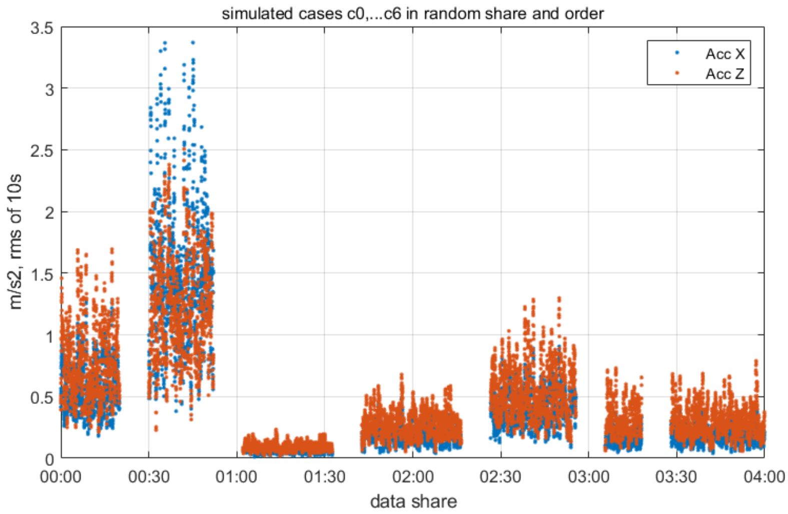

Figure 3-5. Vibration acceleration moving RMS values of 10 s in lateral (X) and vertical (Y) direction.

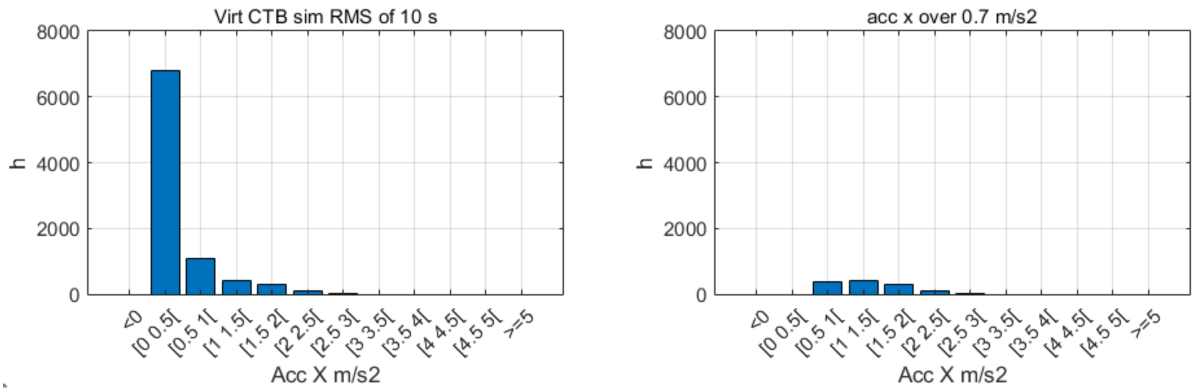

Figure 3-6. TAL values over RMS vibration level classes in lateral direction in total (on left) and when the lateral vibration acceleration RMS has been over operation criteria (over 0.7 m/s2) (on right)

This project has received funding from the European Union's Horizon 2020 research and innovation programme, under the Grant Agreement no. 871571.

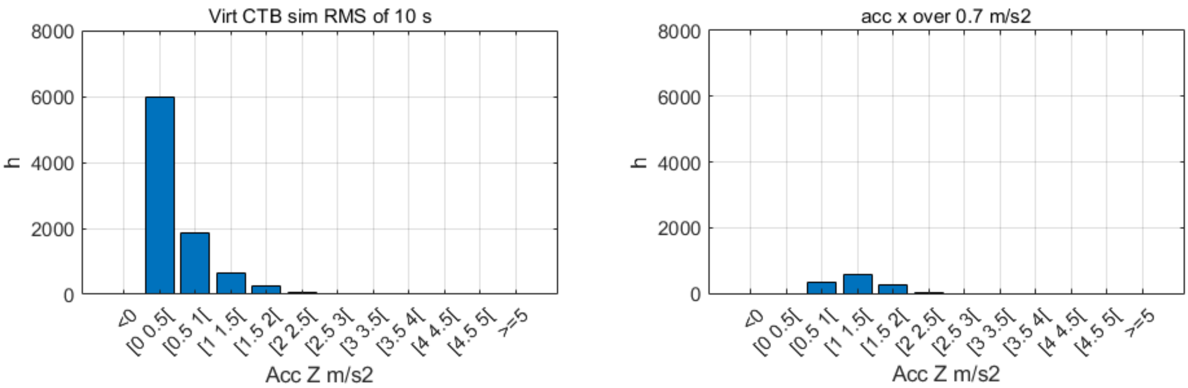

Figure 3-7. TAL values over RMS vibration level classes in vertical direction in total (on left) and when the lateral vibration acceleration RMS has been over operation criteria (over 0.7 m/s2) (on right).

In both cases (shown in Figure 3-6 and Figure 3-7), the weather window during the selected year for possible deployment of human-based maintenance activities has been 86% and respectively the weather downtime has been 14% when evaluated against lateral vibration limits.

3.1.3.2. Inclination based analysis

Respectively, other factors that could be limiting the execution of marine maintenance tasks, can be profiled with TAL. Next, virtual model simulated roll inclination responses are profiled with TAL. According to Table 3-1, the inclination RMS conditions that are greater than 4° are here classified as non-workable marine condition. The inclination data is composed of the simulated responses for cases presented in Table 3-5, as was done with the vibration acceleration evaluations. Figure 3-8 presents a composed inclination data case containing three hours of data, and its moving RMS values of 10 s in given in Figure 3-9. Between each case there is a 10 min time gap for the purpose of separating the cases. These gap segments are not used for TAL profiling.

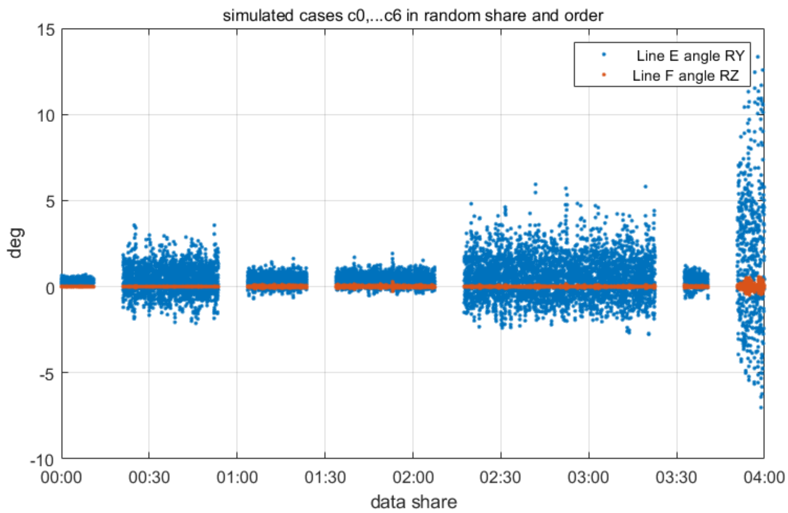

Figure 3-8. Data case representing simulated inclination around lateral (pitch RY) and vertical (yaw Z) axis composed of short duration data segments from all the cases (cases 0 to 6). Here the order and share of the cases are: c6 0.06, c2 0.18, c3 0.11, c4 0.19, c1 0.36, c5 0.05 and c0 0.05.

This project has received funding from the European Union's Horizon 2020 research and innovation programme, under the Grant Agreement no. 871571.

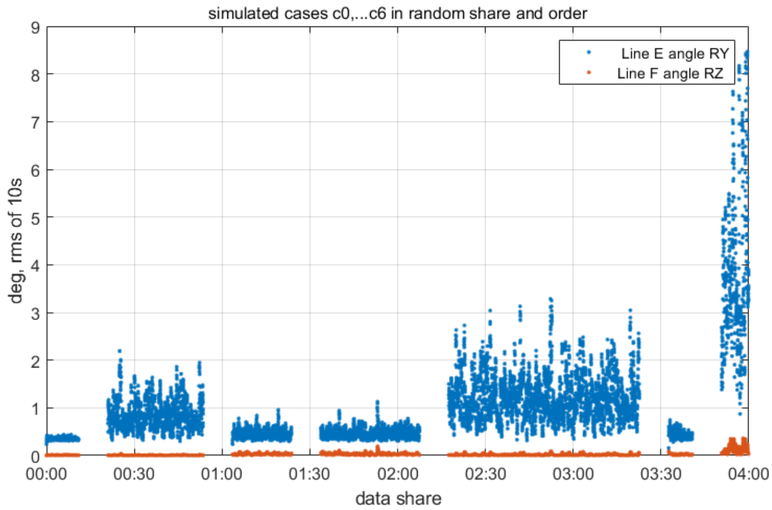

Figure 3-9. Inclination moving RMS values of 10 s in pitch (RY) and yaw (RZ) directions.

The simulated inclination data set was composed of all cases as was done with the vibration acceleration TAL studies shown earlier: the 3 h inclination data was repeated consecutively into a dataset lasting a year (8760 h). However, here the share of the cases is not equal to vibration cases, thus representing a different case for marine weather window evaluations. TAL values profiled to the example inclination data (see Figure 3-9) are shown in pitch directions in Figure 3-10 and in yaw direction in Figure 3-11.

When observed through the inclination criteria in pitch (RY) direction, as shown in Figure 3-10 and Figure 3-11, the weather window during the simulated year wise case for possible deployment of human-based maintenance activities has been 98% and respectively the weather downtime only 2%. In addition, it can be seen from Figure 3-11, that RMS of yaw has been between 0 and 1 degrees.

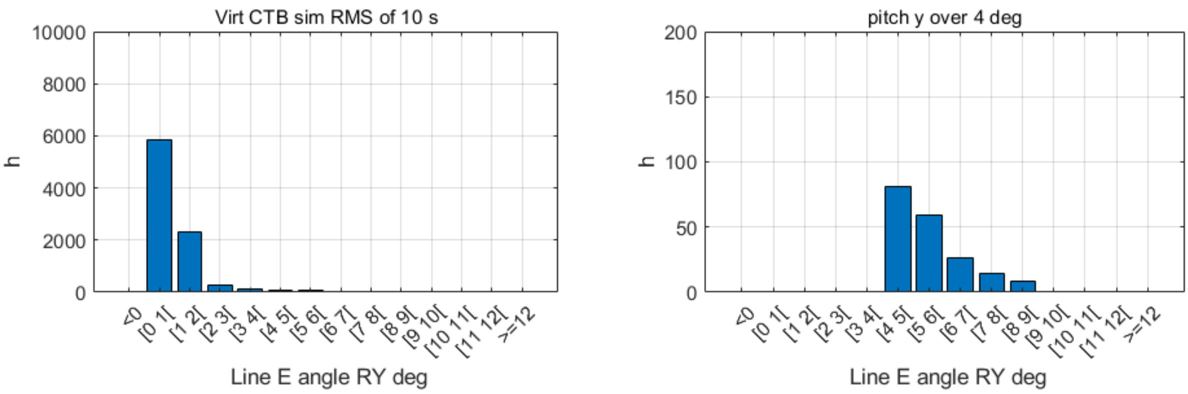

Figure 3-10. TAL values over inclination RMS level classes in pitch direction in total (on left) and when the pitch RMS has been over operation criteria (over 4 degrees) (on right).

This project has received funding from the European Union’s Horizon 2020 research and innovation programme, under the Grant Agreement no. 871571.

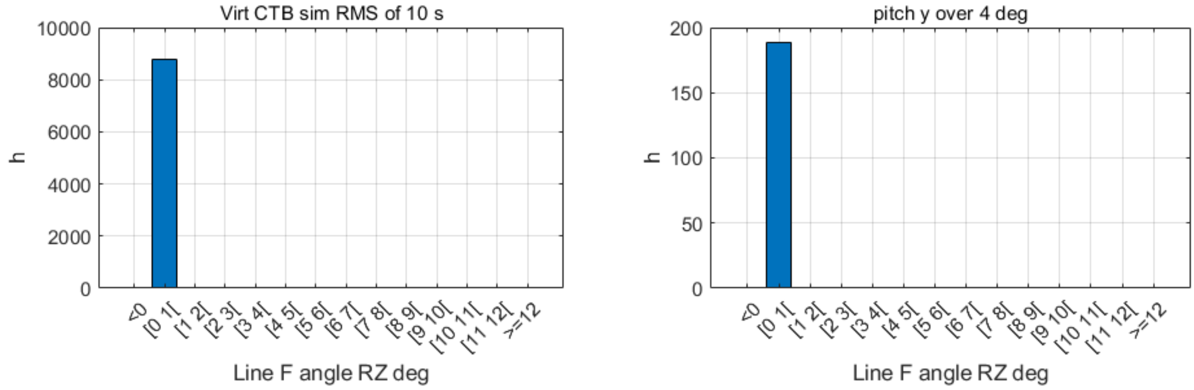

Figure 3-11. TAL values over inclination RMS level classes in yaw direction in total (on left) and when the pitch RMS has been over operation criteria (over 4 degree) (on right).

3.1.3.3. Vibration based analysis with additional data

After the presented year wise results, the next month might be totally different from the previous year, e.g. if more heavy weather conditions are prognosed for the coming month, the weather windows will be totally different since the situation varies all the time in practice. Figure 3-12 and Figure 3-13 present heavy conditions, where the segment share for the extreme conditions lasts longer.

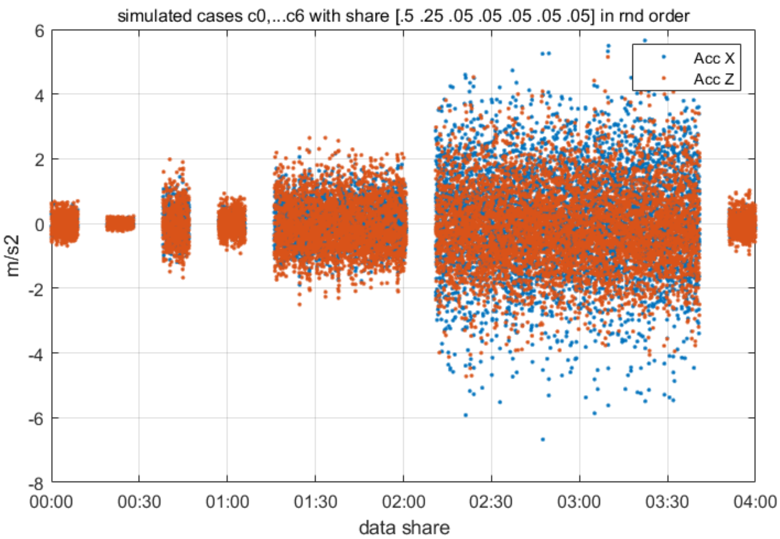

Figure 3-12. Data case representing simulated vibration acceleration in lateral (X) and vertical (Z) direction composed of short duration data segments from all the cases from cases 0 to 6. The order and share of the cases are: c5 0.05, c6 0.05, c2 0.05, c4 0.05, c5 0.25, c0 0.5 and c3 0.05

This project has received funding from the European Union's Horizon 2020 research and innovation programme, under the Grant Agreement no. 871571.

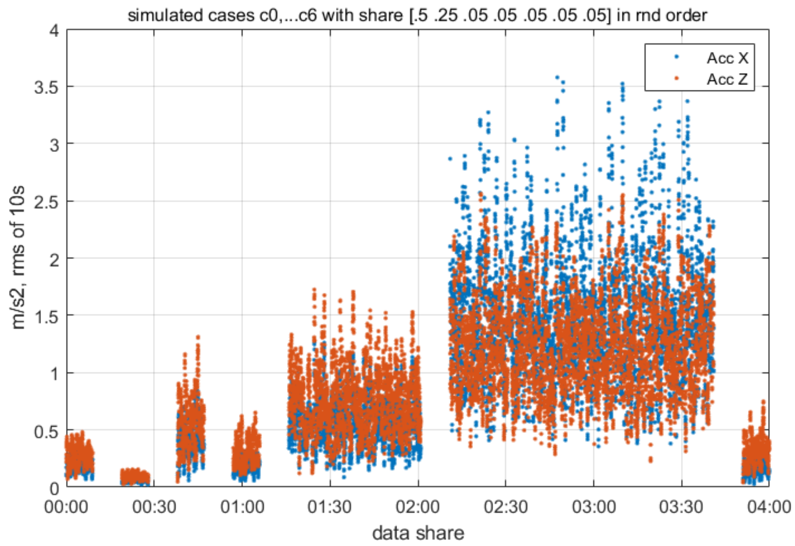

Figure 3-13. Data case vvibration acceleration moving RMS values of 10 s in lateral (X) and vertical (Y) direction.

For the generation of TAL profiles for the extra months the composed 3 h data was first repeated consecutively into a dataset lasting one month (720 h). Figure 3-14 shows TAL values profiled to the example vibration acceleration data (Figure 3-13) in lateral direction and Figure 3-15 in vertical direction.

In the both cases shown in Figure 3-14 and Figure 3-15, the weather window during the selected month for possible deployment of human-based maintenance activities has now been only 46% and respectively weather downtime has been 54% when evaluated against lateral vibration limits.

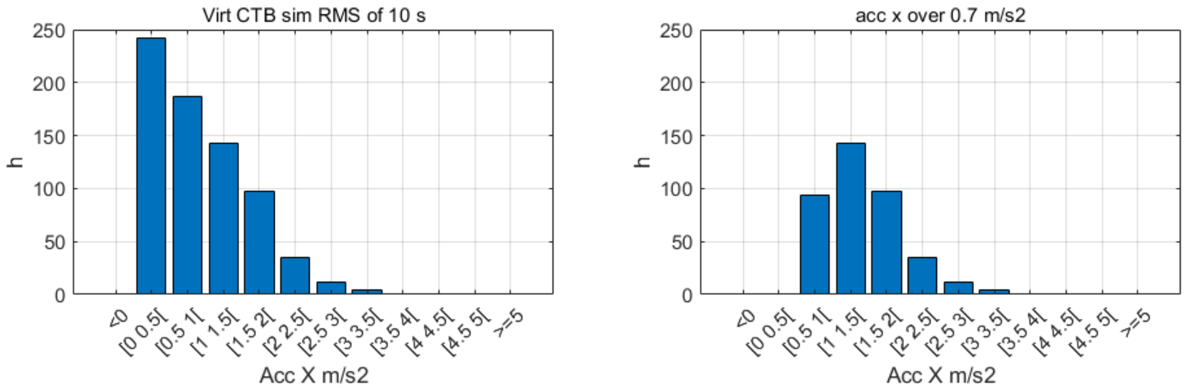

Figure 3-14. TAL values over RMS vibration level classes in lateral direction in total (on left) and when the lateral vibration acceleration RMS has been over operation criteria (over 0.7 m/s2) (on right). Data representing profiles over a simulated heavy month case

This project has received funding from the European Union's Horizon 2020 research and innovation programme, under the Grant Agreement no. 871571.

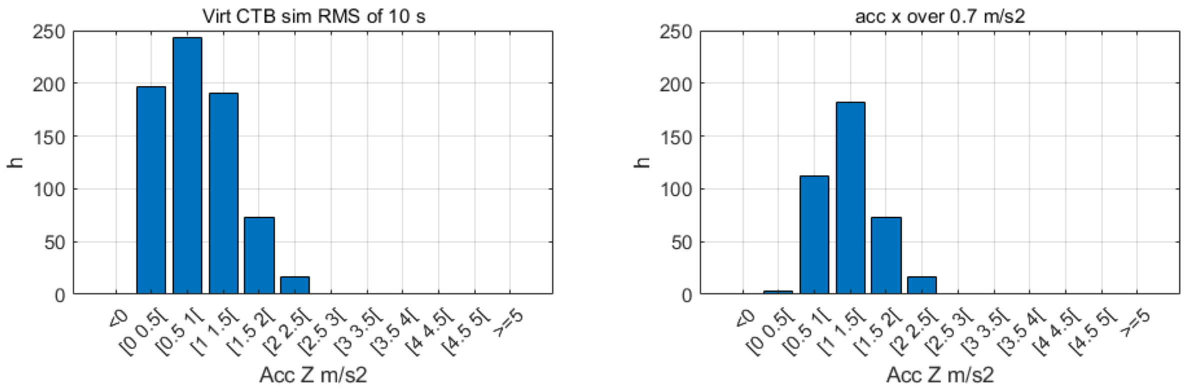

Figure 3-15. TAL values over RMS vibration level classes in vertical direction in total (on left) and when the lateral vibration acceleration RMS has been over operation criteria (over 0.7 m/s2) (on right). Data representing profiles over a simulated heavy month case.

If the month-wise heavy case is added to the existing TAL profiles (lasting one year) the outcome is presented in Figure 3-16 and Figure 3-17.

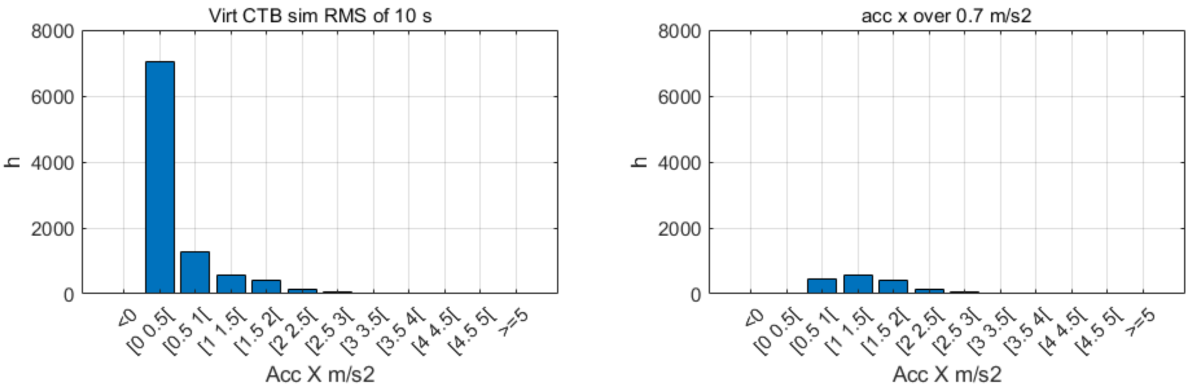

Figure 3-16. TAL values over RMS vibration level classes in lateral direction in total (on left) and when the lateral vibration acceleration RMS has been over operation criteria (over 0.7 m/s2) (on right). Data representing profiles over a simulated year and one month.

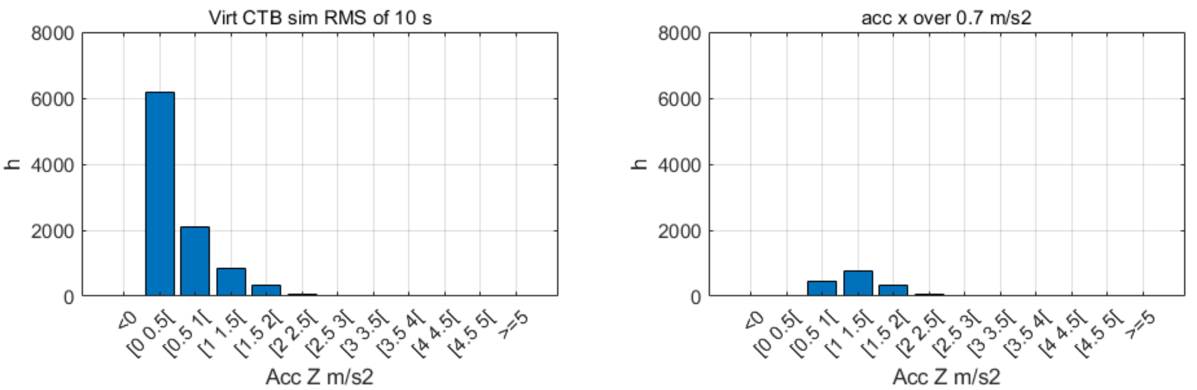

Figure 3-17. TAL values over RMS vibration level classes in vertical direction in total (on left) and when the lateral vibration acceleration RMS has been over operation criteria (over 0.7 m/s2) (on right). Data representing profiles over a simulated year and one month.

This project has received funding from the European Union's Horizon 2020 research and innovation programme, under the Grant Agreement no. 871571.

In this summed up case the weather windows covering a year and one month have been changed to 83% and the weather downtime to 17% when evaluated against lateral vibration limits.

These different length analyses can generate useful information when there are coming requirements for maintenance that need to be scheduled based on the prognosed weather conditions: should those be done in earlier stage or after the expected heavy weather conditions. And, when compared with the other units for the global service business and their maintenance planning.

Further on, respective short-term analysis can be made based on the current environmental status at the production site to evaluate probability for maintenance weather window, and the suitability for maintenance personnel deployment based on human operation criteria. Figure 3-18 shows one example based on lateral vibration severity levels.

In addition, different categories can be used to evaluate requirements: what level of sea-experienced personnel is needed related to the expected seafaring, or if there is a need for less demanding marine work, e.g. light manual work to which there is a possibility to apply less strict or different criteria, or if the criteria is related to exposure time e.g. a two hours exposure period etc. (Nordforsk, 1987).

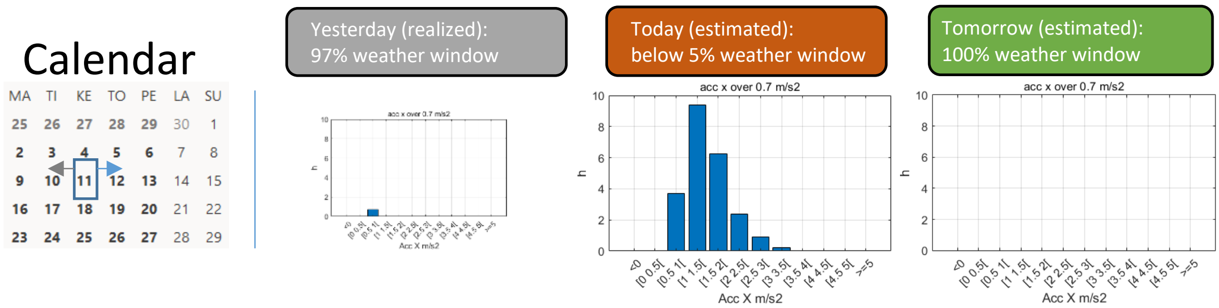

Figure 3-18. Use example for short term weather window estimation using TAL profiling and criteria for later vibrations.

This project has received funding from the European Union's Horizon 2020 research and innovation programme, under the Grant Agreement no. 871571.

3.2. Load analysis for maintenance need assessment

3.2.1. Structural loads

The connection between the mooring lines and the buoy is the location where the structure experiences higher time-varying loads applied to a small area, according to the wave conditions. This way, in the context of this work, the mooring loads are the most relevant from the structural perspective and can be used to assess loading cycles and estimate the required period between maintenances.

The frequency domain analysis done in the previous section defined the most critical wave condition to be used during structural analysis (Table 3-7).

The time domain simulation was conducted over a period of 3 hours or 10800 second, utilizing a time step of 1 second. Figure 3-19Figure 319 - Wave Spectrum for Time Domain Simulation shows the wave spectrum utilized during the simulation.

Comparing the root mean square (RMS) values obtained from the simulation as defined by

$$Deviation = Time\ Domain - Frequency\ Domain \qquad [3]$$

it is noticeable that Time Domain results have minimal difference when compared to the Frequency Domain outcomes for most variables, see Table 3-8. The difference for roll was 0.25 degrees, and for accelerations in X, Y and Z directions, the difference was -0.16, 0.006 and -0.05 m/s^2. Only pitch shows noteworthy deviation, with a value approximately 4.5 degrees lower than that obtained in the frequency domain.

Table 3-7. Wave conditions for structural analysis.

Wave Direction	**degrees**	0
Significant Wave Height (Hs)	**m**	11.5
Peak Period (Tp)	**s**	12
Wave Spectrum	**-**	Jonswap

This project has received funding from the European Union's Horizon 2020 research and innovation programme, under the Grant Agreement no. 871571.

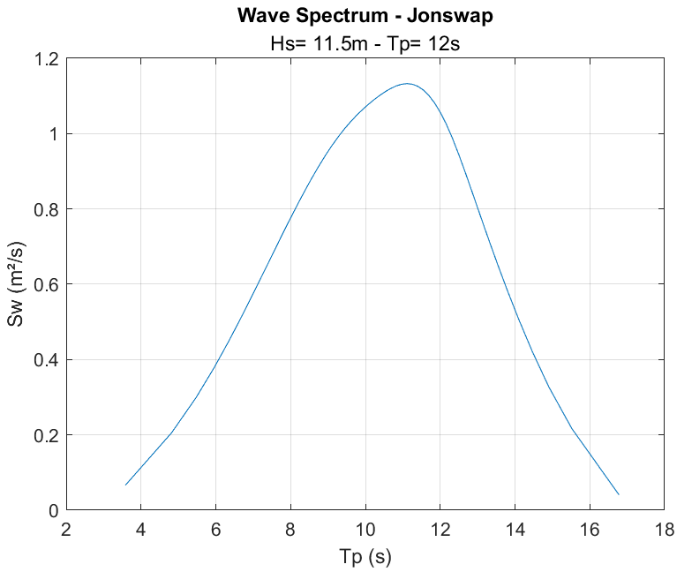

Figure 319 - Wave Spectrum for Time Domain Simulation

Regarding cable tensions, the values acquired in the frequency domain were lower for all three cables. Cable 2 remained as the primary line bearing the heaviest load, with a 17% increase compared to the frequency domain, while the two secondary cables experienced an approximate 63% increase in load. The discrepancy is defined by Equation 4:

$$Discrepancy(\%) = \frac{Frequency\ Domain - Time\ Domain}{Time\ Domain} x\ 100\% \quad [4]$$

Figure 3-20 shows the time series of the cables tension for the simulated scenario.

Table 3-8. Comparison of motions between Frequency and Time Domain

		Frequency Domain	Time Domain	Deviation
RMS Roll	**degrees**	1.06E-03	0.26	0.25
RMS Pitch	**degrees**	8.96	4.47	-4.49
RMS Lat. Acc X	**m/s^2**	1.71	1.55	-0.16
RMS Lat. Acc Y	**m/s^2**	2.30E-04	5.87E-03	0.006
RMS Vert. Acc Z	**m/s^2**	1.35	1.30	-0.05

Table 3-9. Comparison of Cables Tension between Frequency and Time Domain

		Frequency Domain	Time Domain	Discrepancy
RMS Cable 1 Tension	**N**	1.69E+05	4.53E+05	-63 %
RMS Cable 2 Tension	**N**	6.67E+05	8.01E+05	-17 %
RMS Cable 3 Tension	**N**	1.69E+05	4.51E+05	-62 %

This project has received funding from the European Union's Horizon 2020 research and innovation programme, under the Grant Agreement no. 871571.

3.2.1. Mooring loads

The loads applied by the mooring lines in the structure can also be analyzed in the frequency domain. The outcomes for each mooring line and wave condition are plotted below in Figure 3-21.

As expected, higher loads are experienced when a wave direction is aligned with one of the mooring lines. This condition is observed for wave direction of 0 degrees (corresponding to the direction of cable 2), peak period of 12 seconds, and wave height of 11.5m, resulting in a value of 1334.7 kN for the RMS of the cable tension. This critical condition was simulated using the time domain module of ANSYS® Aqwa.

This project has received funding from the European Union's Horizon 2020 research and innovation programme, under the Grant Agreement no. 871571.

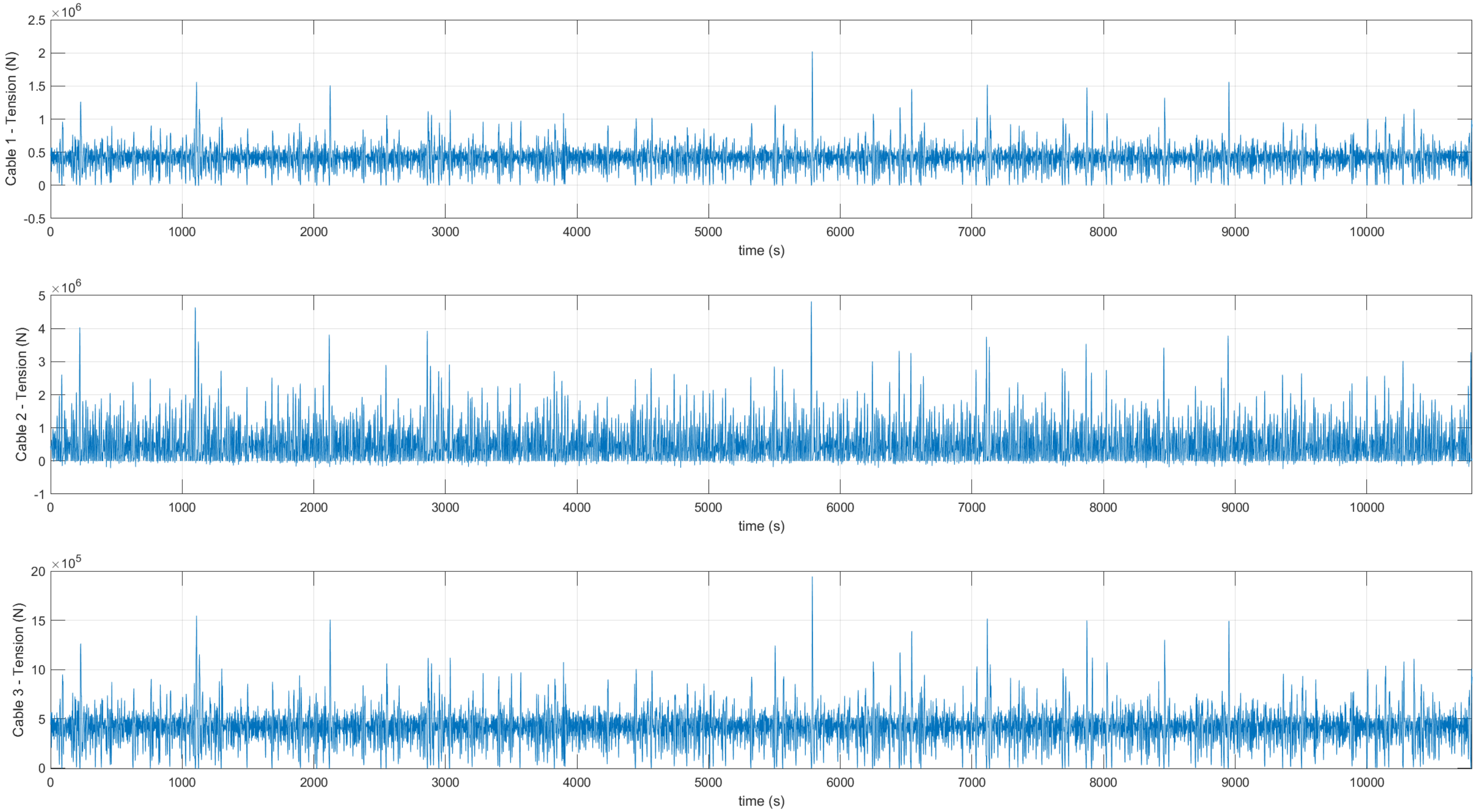

Figure 3-20. Cable tension in time domain.

This project has received funding from the European Union's Horizon 2020 research and innovation programme, under the Grant Agreement no. 871571.

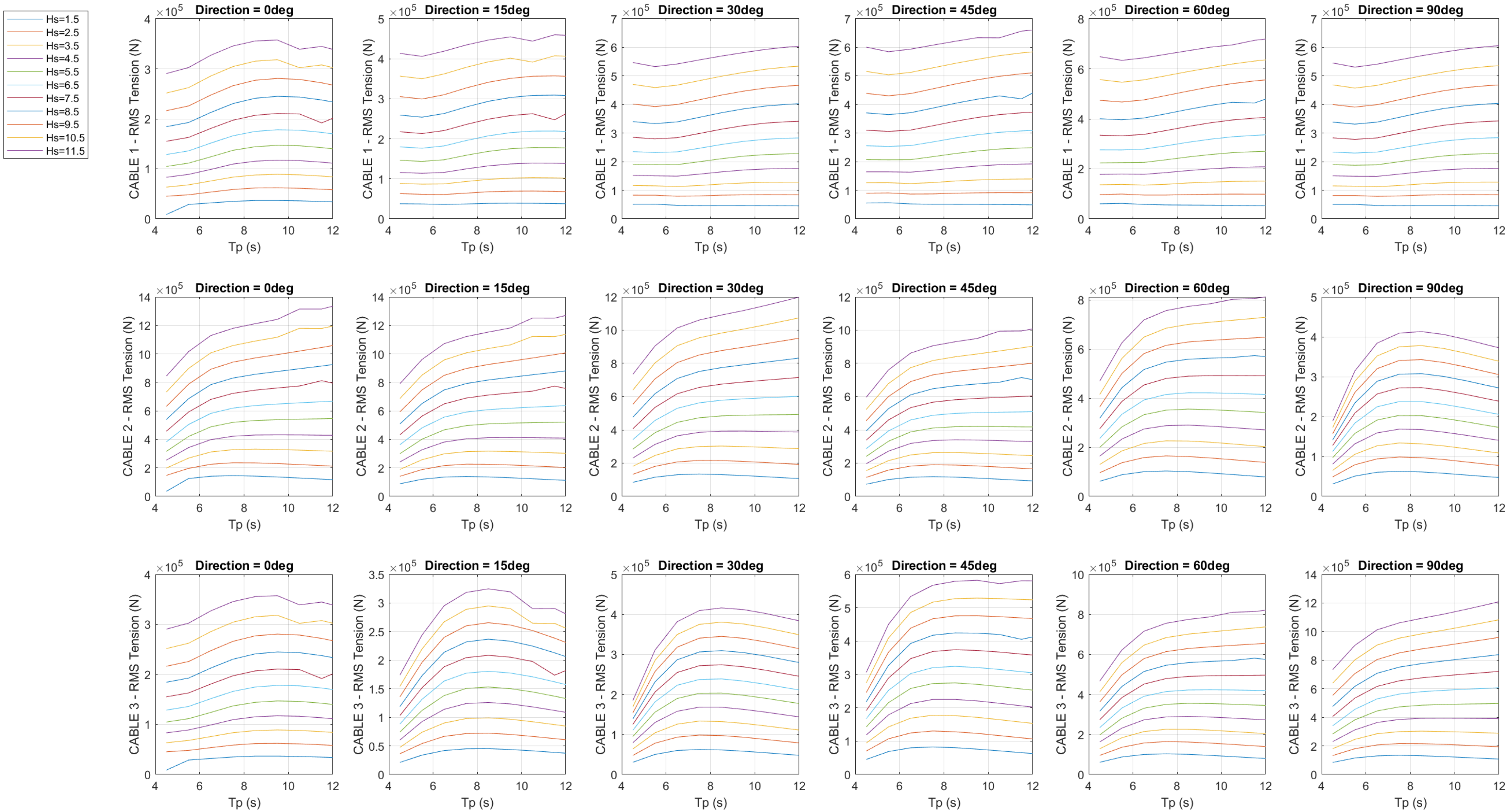

Figure 3-21. Mooring line RMS tension for all three cables for different wave heights (Hs) and directions as a function of peak period (Tp).

This project has received funding from the European Union's Horizon 2020 research and innovation programme, under the Grant Agreement no. 871571.

3.2.2. Mooring line lifetime and maintenance need assessment

Operation environment and realized loading conditions have an effect to the lifetime. Design lifetime can be e.g. over 20 years, and site specific conditions must not have a negative effect to the target design lifetime. In addition to lifetime, inspection and maintenance activities are needed to be carried out every now and then to keep the systems up and running according to reliability requirements and safety rules. In maintenance there are different strategies that could be applied. Traditionally maintenance can be divided into reactive and proactive maintenance. The reactive maintenance is kind of running into a failure and do the repair work after the failure. Proactive maintenance is targeting to prevent the looming failures and anomalies e.g. by predetermined, condition based or predictive maintenance (PdM). In areas with high-capital costs, predictive maintenance has been a next step in managing rising equipment maintenance costs. Naturally, the choice of the best strategy depends on multiple factors, but typically the more critical and expensive the failure causes are, the more justified it is to apply predictive measures. Also accessibility for maintenance is an important affecting factor especially in remote and offshore applications.

Here virtual CTB model simulations responses are used to demonstrate the loading effect on the mooring line. Typically, the effect of loading kind of structural burden is measured best with strain gauges on the critical points. However, e.g. due to the dynamics of the masses, the effect of the loading can be also measured with other means. Anyway, the repeated load or stress variations – if over certain limit – can cause structural damage in materials and the remaining lifetime can be estimated by counting these load cycles. It is typical that the loadings leading to fatigue often vary significantly depending on the operational state and environmental condition. This can be monitored by counting the load cycles for different operational states separately. For this, simulated mooring line loadings are used and the loading cases are composed from the cases shown in Table 3-6 similarly as was done with TAL discussed in Chapter 3.1.3.

The demonstrated load counting method is load level crossing. There are other methods that could be used, like rainflow cycle counting, but the level crossing method is indicative enough to show the effect of load monitoring. The level crossing method records the number of transitions between different loading regions, and the level crossing distribution indicates how much variation occurs at different load levels. Further on, the levels and count numbers are updated to load ranges and cycles (E1049-85, 2017) more suitable for fatigue analysis.

Figure 3-22 presents a data case composed of simulated mooring cable loadings for cable line B and C. This example case contains three hours of data, and is repeated here for the sake of the simplicity as such to last for one year exposure.

This project has received funding from the European Union's Horizon 2020 research and innovation programme, under the Grant Agreement no. 871571.

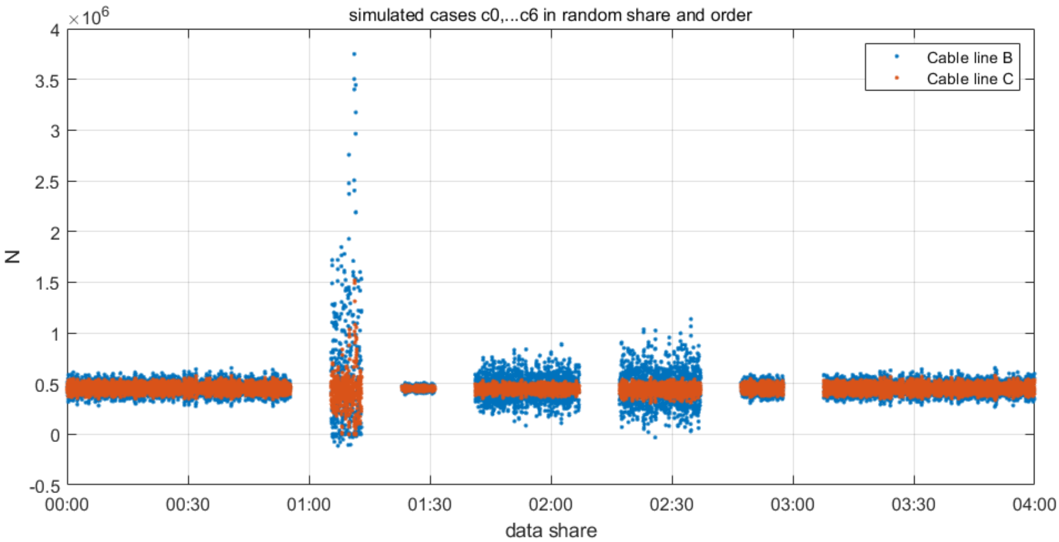

Figure 3-22. Data case representing simulated mooring cable loadings in cable line B and C composed of short duration data segments from all the cases (cases 0 to 6). The order and share (percentage) of the cases are: c5 0.31, c0 0.04, c6 0.05, c2 0.14, c1 0.11, c4 0.06 and c3 0.29

The raw mooring load data for cable B and C are used to calculate cycles for 9 different load ranges. The response is presented in Figure 3-23 and Figure 3-24.

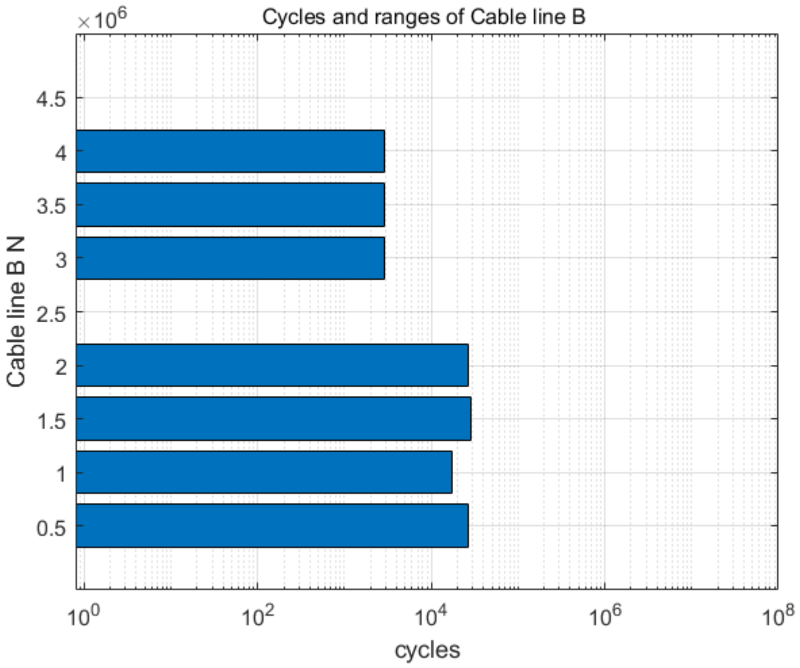

Figure 3-23 Accumulated load range cycles for simulated cable B loadings during one year. The nine load ranges were 0.5, 1, 1.5, 2, 2.5, 3, 3.5, 4 and 4.5 MN.

This project has received funding from the European Union's Horizon 2020 research and innovation programme, under the Grant Agreement no. 871571.

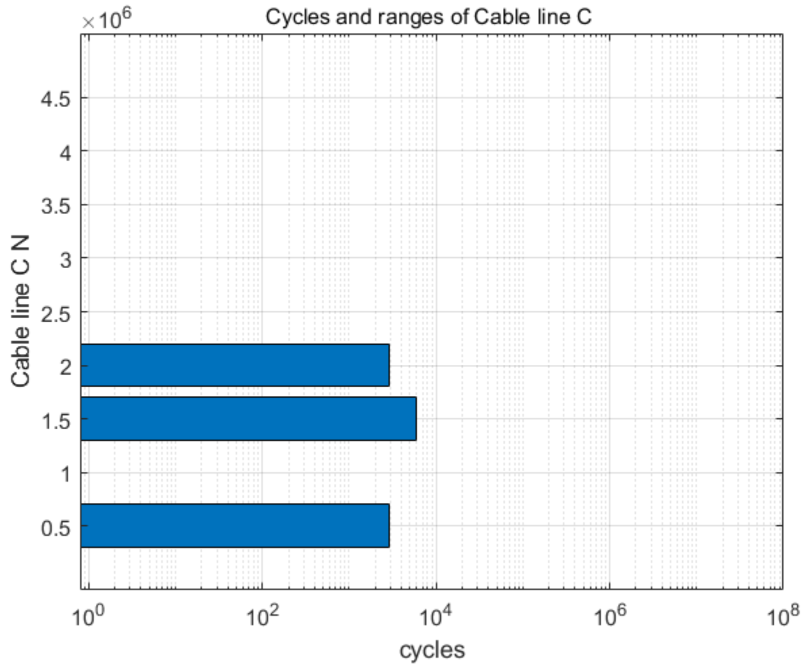

Figure 3-24. Accumulated load range cycles for simulated cable C loadings during one year. The nine load ranges were 0.5, 1, 1.5, 2, 2.5, 3, 3.5, 4 and 4.5 MN.

It can be clearly seen that for this simulated environmental loading case that cable B is carrying higher burden than cable C.

In addition to direct comparisons of the accumulated graphical responses, load cycle counting can be referred to for determining the computational life before failure or e.g. computational time until the next maintenance with the customized Miner's rule which is summing up individual damaging parts. In Miner's rule the total sum of these must be less or equal to 0.5-1, depending on the case and its severity (ISO-6336-6:2006). Here we use 0.5.

$$\text{U} = \sum_i \frac{n_i}{N_i} \leq \ 0.5 \qquad [5]$$

In Equation 5, n_i is cycle count for each load range and N_i is the limiting damage number for each range. N_i can be applied from any practical range-cycle curves. E.g. for stress-cycles there are e.g. Wohler curves which can be used for lifetime analysis. Since in here we do not analyze the loadings as stresses but loading ranges, and we do not know exact lifetime limiting rules or rules for maintenance intervals set e.g. by classification societies, we demonstrate the use of the limits as a fictive example. For that we first define the total limiting number of cycles for each range. Those are presented in Table 3-10.

Here the lowest limiting load range is 1.5 MN, thus infinite number of cycles for the load ranges below 1.5 MN are allowed. Table 3-10 is applied for both cable B and C cases, as shown in Figure 3-25.

Table 3-10. Load ranges and limiting cycles for maintenance inspection.

Case	1	2	3	4	5	6	7	8	9
Load range [MN]	0.5	1	1.5	2	2.5	3	3.5	4	4.5
Limiting mega cycles N []	inf	inf	1	0.42	0.22	0.13	0.08	0.05	0.04

This project has received funding from the European Union's Horizon 2020 research and innovation programme, under the Grant Agreement no. 871571.

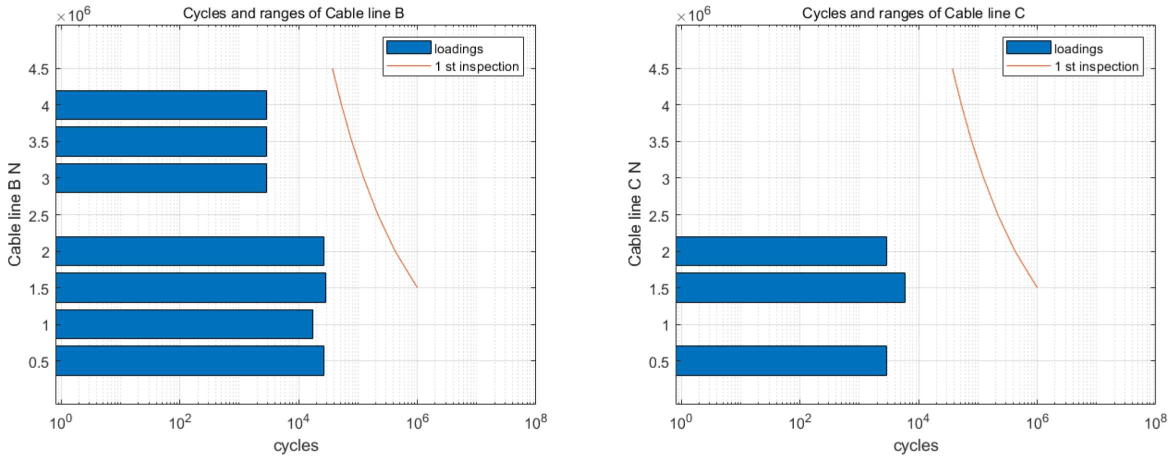

Figure 3-25. Accumulated load range cycles for simulated cable B (on left) and C (on right) loadings during one year with the limiting cycle curves according to Table 3-10 for the first maintenance inspection.

In this example, the total sum for the first inspection is 0.2073 for the cable B and 0.0128 for cable C. Please note the difference in magnitude compared with just the visual comparison of accumulated load cycles graphics. Since the data covers in both cases a period of one year, based on the above presented customized Miner's rule it is about one year until the first inspection for cable B and as much as 38 years for cable C - if the environmental circumstances remain the same as used for the simulation. Please note though that there are additional known factors, which will affect the accumulation for the mooring cable loadings, like how the possible vessel operations and boat moorings affect individual cables. Also, marine growth on the structure and mooring lines and their cleaning intervals will naturally affect the loadings.

This project has received funding from the European Union's Horizon 2020 research and innovation programme, under the Grant Agreement no. 871571.

4. The O&M toolbox as a part of robotic-based IMR

The presented approach can be applied for the deployment of IMR robots for various activities such as condition verification and cleaning surfaces from marine growth. Further on, the analysis can be used to give feedback to operators, R&D personnel, work planning and maintenance management about the real burden of the critical parts - demonstrated here for the mooring lines. In the applied approach, the developed virtual model is used as an indistinguishable digital counterpart of the physical ATLANTIS Coastal Testbed (CTB). The virtual part is used for system simulations, and for testing and surveying immediate and future effects that might be critical for operation and maintenance. The virtual and physical parts are connected through the Operation and Maintenance (O&M) module and the Supervisory Control Centre (SCC) as shown in Figure 4-1.

Based on physical measured responses and/or simulation generated data, the O&M tools are used to carry out short-term and long-term structural loading analysis and to evaluate the operation criteria either in real-time or for future/anticipated weather and sea state conditions. From the O&M part the processed state and operation information is fed to SCC for maintenance planning and decision support for IMR robot deployment. Based on the IMR mission results, the mission feedback can be used for the planning of the future missions and needs. Further on, possible updated needs from the IMR activity outcome can be used as initial information for targeted simulation requests. In the presented loop, the change in state of the physical CTB can lead to a change of state in the virtual model, and the virtual model output can generate a change in the CTB, thus the concept isin bidirectional, as required for a digital twin.

The presented approach utilizing digital twin model of the CTB, the O&M toolbox and the SCC makes it possible to transform the IMR activities from reactive to proactive. It enables making the observations, inspection robot deployment and maintenance activities as condition based instead of simply calendar or accumulated time based.

This project has received funding from the European Union’s Horizon 2020 research and innovation programme, under the Grant Agreement no. 871571.

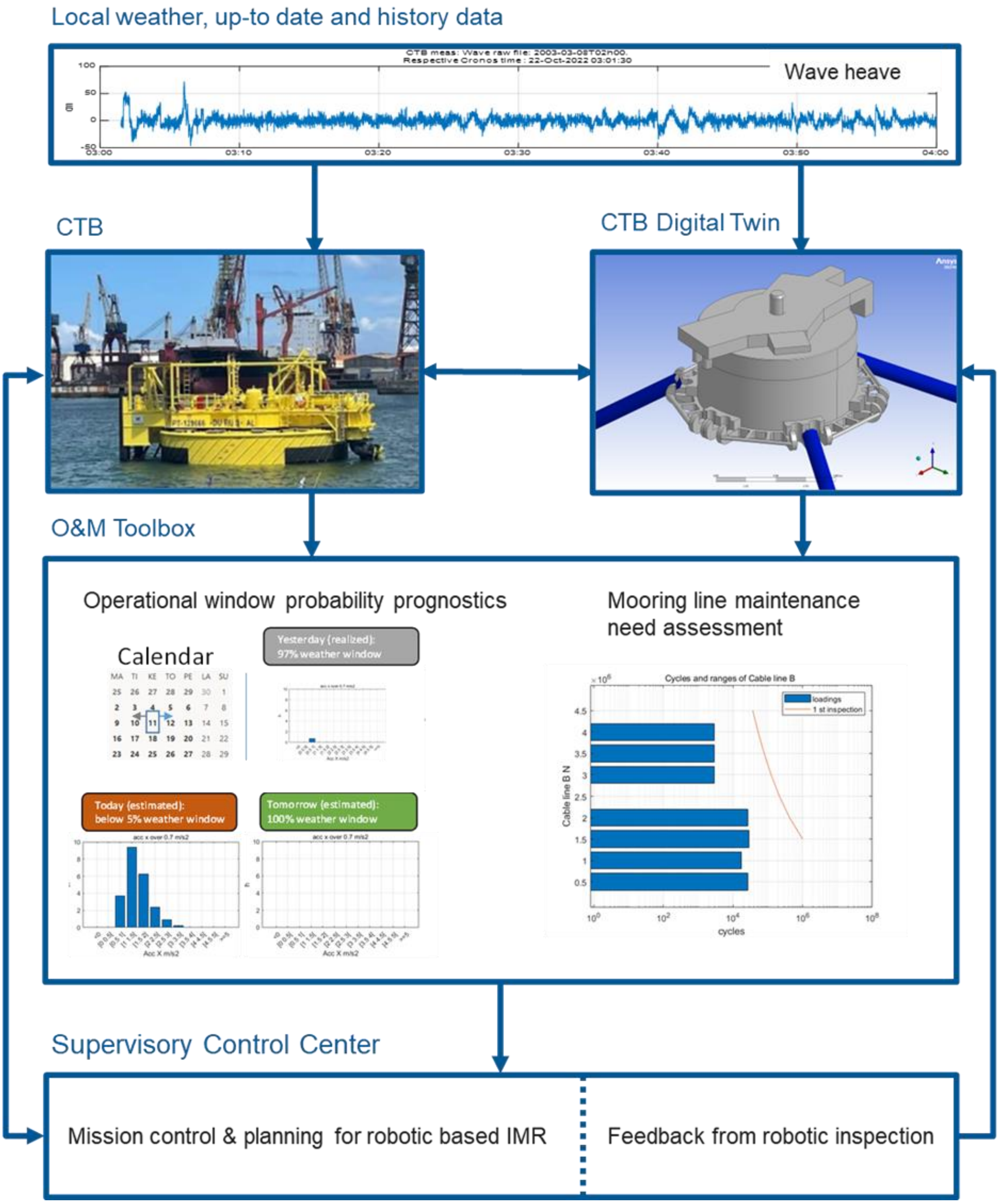

Figure 4-1. Information flow between external data, the CTB, the CTB Digital Twin, the O&M toolbox and the SCC.

This project has received funding from the European Union's Horizon 2020 research and innovation programme, under the Grant Agreement no. 871571.

5. Conclusions

The ATLANTIS Coastal Testbed structure was measured dynamically and statistically over local wave and wind conditions at the harbour in Viana do Castelo, Portugal. Based on the excitation and response data, and main structural dimensions, a virtual model of the ATLANTIS Coastal Testbed was built. The model was used for further operational analysis and maintenance evaluations under conditions that represent conditions at the Atlantic Ocean on the coast of Portugal and that are similar to the conditions at the ATLANTIS Offshore Testbed.

The data simulated with the virtual model were tested for operational window and mooring line maintenance need assessments. It is shown how data can be used to

a) determine operational window for human and robotic-based inspections utilizing motions of the structure, and

b) provide deterministic decision-making support for deployment of robots for targeted and justified inspections.

The operational window analysis was demonstrated by counting the time spent in different operating regions, and the support for inspection deployment was demonstrated by counting first the loads within defined loading ranges, which were then further transformed to computational time until the next inspection/maintenance . The effect was shown in different marine sea state conditions.

Adaptation of the demonstrated methods could help the operator to take actions to execute justified inspections and to prevent faults, and thus reduce the maintenance costs. The methods can be also used for flagging e.g. sea state conditions leading to premature failures and reduced lifetime.

This project has received funding from the European Union’s Horizon 2020 research and innovation programme, under the Grant Agreement no. 871571.

References

61400-3-1:2019-04., I. s. (n.d.). Wind energy generation systems –Part 3-1: Design requirements for fixed offshore wind turbines.

Ansys®Aqwa, Release 2023 R2, Help System, ANSYS, Inc. (2023).

Azcona, J., & Vittori, F. (2019). Mooring System Design for the 10MW Triple Spar Floating Wind Turbine at a 180m Sea Depth Location. *Journal of Physics*.

British Maritime Technology. (1986). Wave Global Statistics. (N. Hogben, N. Dacunha, & G. Oliver, Eds.)

E1049-85, A. (2017). Standard Practices for Cycle Counting in Fatigue Analysis DOI: 10.1520/E1049-85R17.

ISO-6336-6:2006, I. s. (n.d.). -Calculation of load capacity of spur and helical gears — Part 6: Calculation of service life under variable load.

Nordforsk. (1987). Assessment of Ship Performance in a Seaway: The Nordic Co-operative Project: "Seakeeping Performance of Ships". 1987. ISBN:8798263714.

This project has received funding from the European Union's Horizon 2020 research and innovation programme, under the Grant Agreement no. 871571.